

November 2016

LIVE LOAD DISTRIBUTION FACTORS FOR HORIZONTALLY CURVED CONCRETE BOX GIRDER BRIDGES

Mohammed Zaki
University of Massachusetts Amherst

Follow this and additional works at: https://scholarworks.umass.edu/masters_theses_2



Part of the [Civil and Environmental Engineering Commons](#)

Recommended Citation

Zaki, Mohammed, "LIVE LOAD DISTRIBUTION FACTORS FOR HORIZONTALLY CURVED CONCRETE BOX GIRDER BRIDGES" (2016). *Masters Theses*. 455.

https://scholarworks.umass.edu/masters_theses_2/455

This Open Access Thesis is brought to you for free and open access by the Dissertations and Theses at ScholarWorks@UMass Amherst. It has been accepted for inclusion in Masters Theses by an authorized administrator of ScholarWorks@UMass Amherst. For more information, please contact scholarworks@library.umass.edu.

**LIVE LOAD DISTRIBUTION FACTORS
FOR HORIZONTALLY CURVED CONCRETE
BOX GIRDER BRIDGES**

A Thesis Presented

by

MOHAMMED AMEEN ZAKI

Submitted to the Graduate School of the
University Of Massachusetts Amherst in partial fulfillment
of the requirement for the degree of

MASTER OF SCIENCE IN CIVIL ENGINEERING

September 2016

Civil and Environmental Engineering

**LIVE LOAD DISTRIBUTION FACTORS
FOR HORIZONTALLY CURVED CONCRETE
BOX GIRDER BRIDGES**

A Thesis Presented

by

MOHAMMED AMEEN ZAKI

Approved as to style and content by:

Sergio F. Breña, Chair

Simos Gerasimidis, Member

Richard N. Palmer, Department Head

Civil and Environmental Engineering Department

ACKNOWLEDGMENTS

I would like to thank and acknowledge all those people who helped make this thesis possible and an unforgettable experience for me.

My deepest appreciation to engineer Zainab Ali Aziz for her help getting me some important information related to my thesis studies and for her support and interest in my research. Without her assistance, I would not have been able to realize this project.

I am grateful to my advisor, Professor Sergio F. Breña, for his guidance and recommendations. Thank you to my friend Alaa Al- Sammari for listening, offering me advice and supporting me throughout this entire process. Special thanks to my friend Marty Klein, for his time and careful attention. Marty, I would like to acknowledge you with gratitude for all your help and guidance throughout my journey. I am blessed to have you as a best friend, one who is always willing to help and support me.

In addition, my gratitude goes to Dr. Hassan Jony, Dr. Ikbal N. Gorgis, and Huda Ismaeel from the University of Technology, Baghdad, for their assistance in this project. Dr Ikbal Gorgis, I really appreciate you sharing your experience and knowledge to guide me in my work. Also, thank you for checking my modeling procedures, providing advice and for your willingness to answer any and all of my structural engineering questions.

In closing, I would like to take this opportunity to express my profound gratitude, from deep in my heart, to my country, Iraq, and to the “Higher Committee for Educational Development in Iraq” (HECD) for their financial support. I wish my country all the best and God bless. And lastly, I am very thankful to my parents, my brothers and sisters for their loving support and for inspiring me to follow my dreams.

ABSTRACT

LIVE LOAD DISTRIBUTION FACTORS FOR HORIZONTALLY CURVED CONCRETE BOX GIRDER BRIDGES

SEPTEMBER 2016

MOHAMMED AMEEN. ZAKI, B.S., UNIVERSITY OF TECHNOLOGY,
BAGHDAD, IRAQ

M.S.C.E, UNIVERSITY OF MASSACHUSETTS AMHERST

Directed by: Professor Sergio F. Breña

Live load distribution factors are used to determine the live-load moment for bridge girder design when a two dimensional analysis is conducted. A simple, analysis of bridge superstructures are considered to determine live-load factors that can be used to analyze different types of bridges. The distribution of the live load factors distributes the effect of loads transversely across the width of the bridge superstructure by proportioning the design lanes to individual girders through the distribution factors.

This research study consists of the determination of live load distribution factors (LLDFs) in both interior and exterior girders for horizontally curved concrete box girder bridges that have central angles, with one span exceeding 34 degrees. This study has been done based on real geometry of bridges designed by a company for different locations. The goal of using real geometry is to achieve more realistic, accurate, and practical results.

Also, in this study, 3-D modeling analyses for different span lengths (80, 90, 100, 115, 120, and 140 ft) have been first conducted for straight bridges, and then the results compared with AASHTO LRFD, 2012 equations. The point of starting with

straight bridges analyses is to get an indication and conception about the LLDF obtained from AASHTO LRFD formulas, 2012 to those obtained from finite element analyses for this type of bridge (Concrete Box Girder). After that, the analyses have been done for curved bridges having central angles with one span exceeding 34 degrees. These analyses conducted for various span lengths that had already been used for straight bridges (80, 90, 100, 115, 120, and 140 ft) with different central angles (5°, 38°, 45°, 50°, 55°, and 60°).

The results of modeling and analyses for straight bridges indicate that the current AASHTO LRFD formulas for box-girder bridges provide a conservative estimate of the design bending moment. For curved bridges, it was observed from a refined analysis that the distribution factor increases as the central angle increases and the current AASHTO LRFD formula is applicable until a central angle of 38° which is a little out of the LRFD's limits.

TABLE OF CONTENTS

	Page
ACKNOWLEDGEMENTS.....	iii
ABSTRACT.....	iv
LIST OF TABLES.....	ix
LIST OF FIGURES.....	xii
CHAPTER	
1 INTRODUCTION.....	1
1.1 Live load Distribution Factors.....	1
1.2 Objective of the Study.....	5
1.3 Selection of Box-Girder Bridges.....	5
1.4 Organization.....	7
2 LITERATURE REVIEW.....	8
2.1 General.....	8
2.2 Background about Live Load Distribution Factor.....	8
2.3 Previous Research Studies.....	9
2.3.1 Khaleel and Itani.....	9
2.3.2 Zokaie, Osterkamp and Imbsen.....	9
2.3.3 Chen and Aswad.....	11
2.3.4 Shahawy and Huang.....	11
2.3.5 Simth D.....	12
2.4 Development of Distribution Factor in AASHTO LRFD.....	12
2.4.1 AASHTO-LRFD Specification.....	12
2.4.2 Procedure of Determining LLDF in AASHTO LRFD.....	13
2.4.3 Identification of Key Parameters.....	14
2.5 Current AASHTO Formulas for Box Girder Bridge.....	15

3	DESCRIPTION OF MODEL BRIDGE AND LIVE LOAD LOADING.....	19
3.1	Selection of the Span Length for the Box Girder Bridge.....	19
3.2	Proposed Bridge Geometry	19
3.3	Description of Finite Element Models.....	21
3.3.1	Boundary Condition of the Bridge Bearing.....	21
3.3.2	Element Type of the Bridge.....	21
3.4	Live Loading.....	22
3.4.1	Traffic Loads.....	22
3.5	One and Two Lane Moments.....	25
4	STRAIGHT BRIDGE MODEL AND ANALYZING.....	30
4.1	Modeling Straight Bridges	30
4.2	Results and Discussions for Straight Bridges	31
4.2.1	Negative Moment (HL-93S).....	33
4.2.2	Positive and Negative Moments (HL-93K)	33
4.2.2.1	Maximum Positive Moment.....	34
4.2.2.2	Maximum Negative Moment.....	34
4.3	Live Load Distribution Factors (LLDF) for Straight Bridges.....	35
4.4	Comparison of the Results for Straight Bridges	37
4.5	Distribution Factor for Entire Bridge.....	42
5	CURVED BRIDGE MODELINGS AND ANALYSES.....	44
5.1	Curved Bridge Restrictions In AASHTO LRFD.....	44
5.2	Description of the Centrifugal Force, CE.....	44
5.3	Braking Force, BR.....	46

5.4	Curved Bridge modeling and Analysis.....	47
5.5	Results and Discussion for Curved Bridges.....	48
5.5.1	Effect of the Curvature.....	48
5.5.2	Effect of Centrifugal and Braking Forces.....	49
5.6	Distribution Factor Results (LLDF) for Central Angle of 5°.....	51
5.7	Comparison of Results for Central Angle of 5°.....	53
5.8	Distribution Factors for Central Angles of 38°, 45°, 50°, 55°, 60°.....	55
5.9	Comparison of Results for Central Angle of 38°, 45°, 50°, 55°, 60°.....	57
5.10	Distribution Factors for the Entire Bridge.....	60
5.11	LLDF Values with the Effects of CE and BR Forces.....	63
6	SUMMARY AND CONCLUSIONS.....	69
6.1	Summary.....	69
6.1.1	Straight Box Girder Bridges.....	69
6.1.2	Curved Box Girder Bridges.....	70
6.2	Conclusions.....	71
6.2.1	Straight Bridge.....	71
6.2.2	Curved Bridge.....	71
	APPENDIX: RESULTS OF MOMENTS	73
	BIBLIOGRAPHY	77

LIST OF TABLES

Table	Page
1.1: LLDF Equations for Moment in Interior and Exterior Girders.....	4
2.1: Formulas for Moment Distribution on Interior Girders.....	16
2.2: Formulas for Moment Distribution in Exterior Girders.....	16
2.3: AASHTO-LRFD Formulas for Moment Distribution in Interior Girders.....	17
2.4: Distribution of Live Load for Moment in Interior Girder, AASHTO LRFD.....	17
2.5: Distribution of Live Load for Moment in Exterior Girder, AASHTO LRFD...	18
3.1: Multiple Presence Factors.....	27
4.1: LLDF for Negative Moment Due to HL-93S- One Lane Loaded.....	35
4.2: LLDF for Negative Moment Due to HL-93S- Two Lanes Loaded.....	35
4.3: LLDF for Positive Moment Due to HL-93K- One Lane Loaded	36
4.4: LLDF for Negative Moment Due to HL-93K- One Lane Loaded.....	36
4.5: LLDF for Positive Moment Due to HL-93K- Two Lanes Loaded.....	36
4.6: LLDF for Negative Moment Due to HL-93K- Two Lanes Loaded.....	37
4.7: Maximum LLDF for Entire Bridge.....	42
5.1: LLDF for HL-93S- One Lane Loaded-Negative Moment.....	51
5.2: LLDF for HL-93S- Two Lanes Loaded-Negative Moment.....	52
5.3: LLDF for HL-93K- One Lane Loaded-Positive Moment.....	52
5.4: LLDF for HL-93K- One Lane Loaded-Negative Moment.....	52
5.5: LLDF for HL-93K- Two Lanes Loaded-Positive Moment.....	53
5.6: LLDF for HL-93K- Two Lanes Loaded-Negative Moment.....	53
5.7: LLDF for Curved Bridge with a Central Angle of 38°.....	55

5.8:	LLDF for Curved Bridge with a Central Angle of 45°	56
5.9:	LLDF for Curved Bridge with a Central Angle of 50°	56
5.10:	LLDF for Curved Bridge with a Central Angle of 55°	57
5.11:	LLDF for Curved Bridge with a Central Angle of 60°	57
5.12:	Maximum LLDF for the Entire Bridge	61
5.13:	Maximum LLDF for the Entire Bridge	61
5.14:	Maximum LLDF for the Entire Bridge	62
5.15:	Maximum LLDF for the Entire Bridge	62
5.16:	Maximum LLDF for the Entire Bridge	63
5.17:	LLDF with a Central Angle of 38° Including CE and BR Force Effects	64
5.18:	LLDF with a central angle of 45° including CE and BR Force Effects	64
5.19:	LLDF with a Central Angle of 50° Including CE and BR Force Effects	65
5.20:	LLDF with a Central Angle of 55° Including CE and BR Force Effects	65
5.21:	LLDF with a Central Angle of 60° Including CE and BR Force Effects	66
A.1:	Results of Negative Moments (Kips-ft) for HL-93S-One Lane Loaded	78
A.2:	Results of Negative Moments (Kips-ft) for HL-93S-Two Lanes Loaded	78
A.3:	Results of Positive Moments (Kips-ft) for HL-93K-One Lane Loaded	78
A.4:	Results of Negative Moments (Kips-ft) for HL-93K-One Lane Loaded	79
A.5:	Results of Positive Moments (Kips-ft) for HL-93K-Two Lanes Loaded	79
A.6:	Results of Negative Moments (Kips-ft) for HL-93K-Two Lanes Loaded	79
A.7:	Results of Negative Moments for Curved Bridges with a Central Angle of 5°	80
A.8:	Results of Negative Moments for Curved Bridges with a Central Angle of 38°	80
A.9:	Results of Negative Moments for Curved Bridges with a Central Angle of 45°	80

A.10:	Results of Negative Moments for Curved Bridges with a Central Angle of 50°.....	81
A.11:	Results of Negative Moments for Curved Bridges with a Central Angle of 55°.....	81
A.12:	Results of Negative Moments for Curved Bridges with a Central Angle of 60°.....	81
A.13:	Results of Negative Moments for Curved Bridges with a Central Angle of 38°.....	82
A.14:	Results of Negative Moments for Curved Bridges with a Central Angle of 45°.....	82
A.15:	Results of Negative Moments for Curved Bridges with a Central Angle of 50°.....	82
A.16:	Results of Negative Moments for Curved Bridges with a Central Angle of 55°.....	83
A.17:	Results of Negative Moments for Curved Bridges with a Central Angle of 60°.....	83

LIST OF FIGURES

Figure	Page
1.1: Interior and Exterior Girders that Carry the Design Vehicular Loads.....	2
3.1: Span Length for Straight Bridge.....	19
3.2: Span Length for Curved Bridge	19
3.3: Real Geometry of the Box Girder for Span Length of 115 ft.....	20
3.4: For the Maximum-Positive Bending Moment Effect	23
3.5: For the Largest Negative Moment Effects in Continues Span Bridges.....	24
3.6: Spacing of the Wheels.....	24
3.7: One Lane Fully Loaded and the Other Lane Unloaded, Right Lane.....	25
3.8: One Lane Fully Loaded and the Other Lane Unloaded, Left Lane.....	26
3.9: Both Lanes Loaded	26
3.10: The Transverse Position of the Trucks.....	28
4.1: 3-D Modeling of the Bridge by Using CSiBridge Program (2015).....	30
4.2: Entire Bridge (80 ft, Two lanes Loaded).....	32
4.3: Entire Bridge (80 ft, Two lanes Loaded).....	32
4.4: HL-93S- One Lane Loaded- Interior Girder.....	37
4.5: HL-93S- One Lane Loaded- Exterior Girder.....	38
4.6: HL-93S- Two Lanes Loaded- Interior Girder.....	38
4.7: HL-93K- One Lane Loaded- Interior Girder (Positive Moment).....	39
4.8: HL-93K- One Lane Loaded- Exterior Girder (Positive Moment).....	39
4.9: HL-93K- One Lane Loaded- Interior Girder (Negative Moment).....	40
4.10: HL-93K- One Lane Loaded- Exterior Girder (Negative Moment).....	40

4.11: HL-93K- Two Lanes Loaded- Interior Girder Positive Moment.....	41
4.12: HL-93K- Two Lanes Loaded- Interior Girder (Negative Moment).....	41
4.13: Maximum LLDF for the Entire Bridge.....	43
5.1: CE Force on Track Moving on Curved Bridge.....	45
5.2: Distance of Centrifugal Force.....	45
5.3: Truck Loads Plus Braking Force.....	46
5.4: Curved Bridges with $\theta > 34^\circ$	47
5.5: Curved Bridges with $\theta > 34^\circ$	47
5.6: HL-93S- Two Lanes Loaded.....	54
5.7: HL-93K- Two Lanes Loaded- Positive Moment.....	54
5.8: HL-93K- Two Lanes Loaded- Negative Moment.....	55
5.9: LLDF for Curved Bridge with a Central Angle of 38°	58
5.10: LLDF for Curved Bridge with a Central Angle of 45°	58
5.11: LLDF for Curved Bridge with a Central Angle of 50°	59
5.12: LLDF for Curved Bridge with a Central Angle of 55°	59
5.13: LLDF for Curved Bridge with a Central Angle of 60°	60
5.14: LLDF for Curved Bridge with a Central Angle of 38°	66
5.15: LLDF for Curved Bridge with a Central Angle of 45°	67
5.16: LLDF for Curved Bridge with a Central Angle of 50°	67
5.17: LLDF for Curved Bridge with a Central Angle of 55°	68
5.18: LLDF for Curved Bridge with a Central Angle of 60°	68
A.1: Description of Interior and Exterior Girders.....	77

CHAPTER 1

INTRODUCTION

1.1 Live Load Distribution Factors

The live load distribution factors (LLDF) described in the AASHTO-LFD specifications had been used for more than 50 years prior to their update in the AASHTO-LRFD Bridge Design Specification. The formulas represented in AASHTO-LFD are based on the girder spacing only and are usually presented as S/D , where S is the spacing and D is a constant based on the bridge type. This method is suited to straight and non-skewed bridges only. While the formulas represented in AASHTO-LRFD are more useful and accurate since they take into account more parameters, such as bridge length, slab thickness, and number of cells for the box girder bridge typ. The change in AASHTO-LRFD equations has generated some interest in the bridge engineering world and has raised some questions. Skewed Bridges will be gained by using AASHTO-LRFD Specification [3].

Live load distribution factors enable engineers to analyze bridge response by treating the longitudinal and transverse effects of wheel loads separately. These factors have simplified the design process by allowing engineers to consider the girder design moment as the static moment caused by AASHTO standard truck or design lane loads, multiplied by the live-load distribution factor calculated through AASHTO LRFD, 4.6.2.2.2b [4]. Fig 1.1 shows the interior and exterior girders that carry the truck loads. The distribution factor decreases when the bridge shares and distributes the load

efficiently among adjacent girders. This leads to a low design moment for a given truck size.

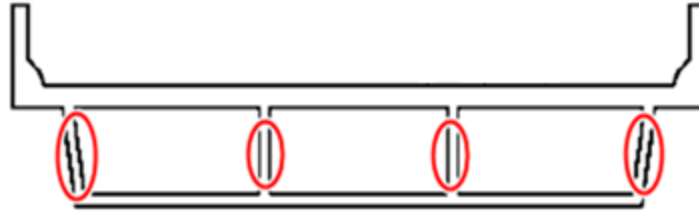


Figure 1.1: Interior and Exterior Girders that Carry the Design Vehicular Loads

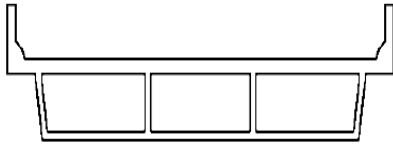
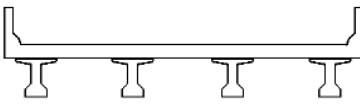
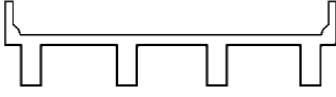
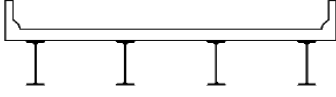
Since 1931, live load distribution factors have been described in the Standard Specification for Highway Bridges. The early values have been updated and modified in 1930 by Westergaard and in 1948 by Newmark as new research results became available. The distribution factor presented in AASHTO Standard Specifications was $S/5.5$ for a bridge constructed with a concrete deck supported on pre-stressed concrete girders. This is applicable for bridges that carry two or more lanes of traffic, where S is the girder spacing in feet. This factor is applied to the moment caused by one line of wheels. Even so, some researchers such as Zokaie have noted that the changes in LLDF over the last 55 years have led to inconsistencies in the load distribution criteria in the Standard Specifications these include: inconsistent changes in distribution factors to reflect changes in design lane width; inconsistent consideration of a reduction in load intensity for multiple lane loading; and inconsistent verification of accuracy of wheel load distribution factors for various bridges [4].

In 1994, AASHTO LRFD Specifications recommended new load distribution equations as an alternative to the Standard Specifications. These distribution equations were derived from the National Cooperative Highway Research program (project 12-26). The formulas consider many bridge parameters including skew and continuity rather than limited parameters that were previously considered in AASHTO Specification. According to Zokaie, the new distribution factors lie within 5 percent of the actual distribution factors found by analyzing the bridge superstructure by using the finite element model.

Although the distribution factor formulas in AASHTO LRFD are considered to be more accurate than the distribution factors in the Standard Specifications, some researchers like Chen and Aswad, have found that they are conservative, and they are uneconomical for bridges with large span –to- depth ratios. According to Chen and Aswad the conservatism of the distribution factors can be 18 to 23 percent for interior girders and 4 to 12 percent for exterior girders [4].

LRFD Article 4.6.2.2.2 presents live load distribution factor formulas for several common types of bridge superstructures. These distribution factors provide a fraction of design lanes that should be used to an individual girder to design it for moment or shear. The factors take into account interaction among loads from multiple lanes. Table 1.1 shows some types of bridge superstructures with equations of live-load distribution factors for moment in interior and exterior girders for different types of straight bridges. There are many other types of bridge superstructures listed in the AASHTO LRFD [1].

Table 1.1: LLDF Equations for Moment in Interior and Exterior Girders

Type of Superstructure	LLDF equations		Range of Applicability
	For Moment in Interior Girders		
Cast-in-Place Concrete Multi-cell Box 	One Design Lane Loaded $(1.75 + S/3.6) (1/L)^{0.35} (1/N_c)^{0.45}$		$7.0 \leq S \leq 13.0$ $60 \leq L \leq 240$ $N_c \geq 3$ If $N_c > 8$ use $N_c = 8$
	Two or More Lanes Loaded $(13/N_c)^{0.3} (S/5.8) (1/L)^{0.25}$		
	For Moment in Exterior Girders		
	One Lane Loaded $g = W_e/14$	Two or More Lanes Loaded $g = W_e/14$	$W_e \leq S$
Precast Concrete I or Bulb-Tee Sections 	One Design Lane Loaded $0.06 + (S/14)^{0.4} (S/L)^{0.3} (Kg/12 Lt_s^3)^{0.1}$		$3.5 \leq S \leq 16.0$ $4.5 \leq t_s \leq 12.0$ $20 \leq L \leq 240$ $N_b \geq 4$ $10,000 \leq Kg \leq 7,000,000$
	Two or More Lanes Loaded $0.075 + (S/9.5)^{0.6} (S/L)^{0.2} (Kg/12 Lt_s^3)^{0.1}$		
Cast-in-Place Concrete Tee Beam 	For Moment in Exterior Girders		$1.0 \leq d_e \leq 5.5$
	One Lane Loaded	Two or More Lanes Loaded	
Cast-in-place concrete slab, precast concrete slab, steel 	Lever Rule	$g = e g_{interior}$ $e = 0.77 + (d_e/9.1)$	

AASHTO LRFD provides formulas to determine live load distribution factors for several common bridge superstructure types. However, there is a restriction of using these equations for curved bridges having central angles that exceed 34 degrees. This research provides a study and modeling analyses for horizontally curved concrete box girder bridges that have a degree of curvature greater than 34 degrees. In addition, this thesis presents a study for curved bridges that took into account the effect of centrifugal and braking forces.

1.2 Objective of the Study

The objective of this study is to calculate live load distribution factors (LLDFs) for interior and exterior girders of horizontally curved concrete box girder bridges that have central angles, within one span exceeding 34 degrees. The geometry that is used in this study based on real geometry used in some bridges. The goal of using real geometry in this study is to obtain more realistic, accurate, and practical results. These results will provide factors that can be used by engineering designers to determine live load distribution factors on any individual required girder on horizontally curved concrete box girder bridges. All straight and curved bridges that used in this study are prismatic in cross section and continuous over the interior support.

1.3 Selection of Box-Girder Bridges

The box-girder bridge is a common structural form in both steel and concrete. The closed section of the box girder, Fig 1.1 makes the bridge superstructure torsionally much stiffer than its open counterpart. This characteristic makes the box girder ideal for bridges that have significant torsion induced by horizontal curvature resulting from roadway

alignments. For example, the box-girder bridge is often used for tightly spaced interchanges that require curved alignments because of its torsional resistance and fine aesthetic qualities [11].

The Box-Girders can be of different forms and geometry. Box girder decks are cast-in-place units that can be constructed to follow any desired alignment in plan, so that straight, skew and curved bridges of various shapes are common in the highway system. The analysis and design of box-girder bridges are very complex because of its three dimensional behavior consisting of torsion, distortion and bending in longitudinal and transverse directions. There are many methods for analysis of box girders. But in most of the methods the exact nature of curved box girders are not taken into account because of the assumptions made in the analysis. The most rigorous way to analyze such a complex system and obtain detailed results is through finite element modeling. The finite-element method by using shell elements may be used for the box-girder bridge [14].

Cast-in-place multi cell concrete box girder bridge types may be designed as whole-width structures. Such cross-sections shall be designed for the live load distribution factors in AASHTO LFRD, Articles 4.6.2.2.2 and 4.6.2.2.3 for interior girders, multiplied by the number of webs. Regardless of the method of analysis used, approximate or refined, exterior girders of multi beam bridges shall not have less resistance than an interior beam. Whole-width design is appropriate for torsionally stiff cross-sections where load-sharing between girders is extremely high and torsional loads are hard to estimate [1].

1.4 Organization

Chapter 2 describes the historical background of the AASHTO wheel load distribution formula and summary of relevant research studies. The development of the new AASHTO-LRFD formulas is then explained based on the NCHRP 12-26 project (Zokaie et al. 2000). The previous and current AASHTO formulas for concrete box girder bridge are also discussed.

Chapter 3 presents the description of model bridge such as the geometry and properties of the box girder bridge and the span length. The live loading, the maximum girder moment based on the AAHTO HL-93 design truck loads are also explained for one and two lanes loaded.

Chapter 4 discusses the results of live load distribution factors for moment in both interior and exterior girders for straight bridges. In addition, the distribution factors for entire bridge are determined and discussed for the box girder according to the AASHTO LRFD, 4.6.2.2.1 and Washington State Department of Transportation, Bridge Design Manual.

Chapter 5 consists of the determination of the distribution factors for curved bridges having different central angles and varies span lengths. In addition, this chapter presents the description and determination of the centrifugal and braking forces. Also, the increase in the results of maximum moment due to the effects of centrifugal braking forces are discussed.

Chapter 6 provides the conclusions of this study for both straight and curved concrete box girders bridges.

CHAPTER 2

LITERATURE REVIEW

2.1 General

Bridge engineers have used the concept of distribution factors to estimate the transverse distribution of live loads since the 1930's. The live load distribution for moment and shear is essential to the design of new bridges and to evaluate the load carrying capacity of existing bridges. Big efforts have been made to develop and simplify the live load distribution equations. Also, many researches have been conducted in order to determine the effect of certain parameters, such as girder spacing, span length, and skew angle. The literature review presented in this chapter summarizes past findings that are relevant to this project and will only cover the following areas: background about previous AASHTO specification and AASHTO LRFD, summary of relevant research studies, AASHTO LRFD development, and current AASHTO formulas for box girder bridge.

2.2 Background about Live Load Distribution Factor

The AASHTO-LRFD live load distribution formulas were derived from the National Cooperative Highway Research Program (NCHRP) 12-26 project and they were entitled "Distribution of Live Loads on Highway Bridges". This project was first proposed in 1985 to improve the accuracy of the earlier equations (S/D formulas) that were described in the Standard AASHTO specifications. Upon review of the S/D formulas, it was found that the S/D formulas were applicable to bridges having typical geometry. For example, the S/D formulas were generating valid results for bridges having

girder spacing near to 6 ft and a span length of about 60 ft. However, the formulas needed to be revised and evaluated to get accuracy [4].

2.3 Previous Research Studies

2.3.1 Khaleel and Itani

In 1990, Khaleel and Itani studied the behavior of continuous slab-on-girder bridges subjected to the AASHTO HS20-44 truck loading with different degrees of skew. In this study, up to 112 continuous bridges were analyzed with five pre-tensioned girders using the finite element method. Varied parameters were taken into account including span length, skew angles, and spacing between the girders. The span lengths varied from 80-120 ft, the angles of skew varied between 0 and 60°, and the girder spacings ranged from 6-9 ft. Khaleel and Itani found that previous load distribution formulas in AASHTO Standard Specifications underestimated the positive bending moment for exterior girders by approximately 28%. The design moment was underestimated by 6-40 percent for an interior girder [9].

2.3.2 Zokaie, Osterkamp and Imbsen

This study focused on evaluating and developing methods for determining live-load distribution factors for several common bridge superstructure types. Different kinds of bridges have been considered in this study such as slab-on- beam bridges; multi-cell, box-girder bridges; and multi-box beam bridges. To investigate the live load distribution factors for each bridge type, three methods of analysis were used for this purpose [10].

1- Level 3, this method was considered to be the most accurate analysis, it included a determination of the live load distribution factors with a detailed finite element modeling of the bridge superstructure (deck). Different finite-element programs were used to analyze the bridges. Shell elements were used to model the deck for slab-on- beam bridges, and beam elements were used to model the girders.

2- Level 2 In this method, design charts and grillages using grid models were used to calculate the live load distribution factors.

3-Level 1 Based on Level 2 and 3 analyses, the analysis in level 1 used simplified formulas to calculate the live-load distribution factors. These formulas were found to be accurate as much as those in the level 2 and 3 analysis for their ranges of applicability. Correction factors were applied to the formulas to consider for the effect of girder location such as exterior or interior girder, skew and continuity as well.

The sensitivity of the live-load distribution factors was also studied for different bridge properties. The average bridge properties were varied for each bridge, and their effects on the distribution factors were analyzed and evaluated. Beam spacing was found to be the most significant property. Also, other parameters like span length, longitudinal stiffness, and transverse stiffness affected the distribution factors [4].

According to the Zokaie`s study in 1991, this research resulted in formulas (Level 1 analysis) for determining live-load distribution that are more accurate than those used in the previous codes. These formulas are simpler, easier to use and are approximately as accurate when compared with the methods used in the level 2 and 3 analysis.

2.3.3 Chen and Aswad

The main goal of this study was to revise and evaluate the accuracy of the formulas for live load distribution in the LRFD Specification in 1994 for modern pre-stressed concrete bridges made of I-girders or spread box girders with high span-to-depth ratios. The results of distribution factors obtained from simplified LRFD method were smaller than those obtained from AASHTO Standard Specifications for interior girders. [5].

The study that has been done by Chen and Aswad [6] showed that a refined method of analysis such as finite element analysis, could reduce the midspan moment for spread-box girder by 18-23% for interior girder and by 4-12% for exterior girder when compared to the AASHTO LRFD. A similar reduction was also shown to exist for I-girders. As a result of this study, it was recommended to use a finite element or grillage analysis for longer span bridges.

2.3.4 Shahawy and Huang

In this study the distribution factors determined first from finite element analyses and then compared to those obtained from AASHTO LRFD equations [1]. It was concluded that the methods presented in the Specifications for determining the live load distribution factors for bridges having two or more lanes loaded are satisfactory. However, if the girder spacing and deck overhang exceed 8 and 3 ft, respectively the errors of up to 30% could be expected. It was also concluded that the AASHTO LRFD load distribution factors for interior and exterior girders of two or more design lanes and for one design lane bridges are too conservative for strength evaluation and rating purposes [7].

2.3.5 Simth, D.

A series of parametric studies have been performed by Smith [8] to modify the live load distribution factor method for the Canadian Highway Bridge Design Code. This research study ended up with a distribution factor method based on dividing the total live load equally between all girders and then applying a modification factor based on the properties of the bridge, including span length, number of lanes loaded, girder location (internal vs. external), girder spacing, and width of the design lane. The new method then was compared to the distribution factor method from the 1996 version of the Canadian Highway Bridge Design Code. A separate modification factor is used for flexure and shear. In general, bridges are divided into two separate types: shallow superstructure and multi-spine bridges. Due to this study a set of equations was developed for flexure and shear for different types of bridges such as multi-cell box girders, slab bridges, and steel grid deck-on-girders [8].

2.4 Development of Distribution Factor in AASHTO LRFD

2.4.1 AASHTO-LRFD Specification

Since the AASHTO-Specification would not be accurate when the bridge parameters were varied (e.g., when relatively short or long bridges were considered), the additional parameters such as span length and stiffness properties must be considered in order to get higher accuracy. As a result, the original formulas were revised by Zokaie [3], to improve their accuracy when applied to the LRFD live loads. These formulas were developed by using several bridge types such as reinforced concrete T-beam, pre-stressed concrete I-girder, and steel I-girder, and multi-cell box girder. Then, their results were

compared using an accurate method in order to evaluate the existing formulas. Finite-element or grillage analysis methods were used for this purpose, and bridge superstructure models were prepared based on geometric parameters and material properties. Then, analytical models were developed for several hundred actual bridge superstructures and the database was prepared for all of these bridges [4].

Zokaie conducted a study to evaluate the existing formulas using actual bridge super structure database to compare the results with the finite element results. The parameters study was also examined by Zokaie using the database to indentify the range and variation of each parameter. Then other procedures were followed to simplify the formulas [3]

2.4.2 Procedure of Determining LLDF in AASHTO LRFD

To carry out a finite-element or grillage analysis of the bridge superstructure, several hundred actual bridge decks were prepared by Zokaie [3]. These bridges were selected randomly from the National Bridge Inventory File (NBIF) and bridge plans were obtained from the state departments of transportation. From those bridge plans many parameters were extracted and were stored in a database to be used in the study. The database contained information that included different types of bridge, span lengths, edge to edge widths, skew angles, number of girders, girder depths, slab thicknesses, overhangs, curb to curb widths, year built, girder eccentricities (distance from centroid of the girder to the mid-height of the slab), girder moments of inertia, and girder areas.

2.4.3 Identification of Key Parameters

The bridge database was studied by Zokaie [3], to classify the range and variation of each parameter. For each parameter, the maximum, minimum, average, and standard deviation was obtained. Several parameters were plotted against each other to determine if those parameters are correlated to each other. . For example, the girder spacing and slab thickness that are considered to be correlated to each other, or for larger span lengths that result in larger moments of inertia and/or girder depths. Also, Zokaie conducted a sensitivity study to identify which parameters have a significant effect on the live load distribution. To calculate the live load distribution factors for shear and moment, a bridge superstructure finite-element model was prepared for the average bridge and loaded with the HS20 truck. The longitudinal stiffness ($K_g = I + Ae^2$) parameter was introduced for the girder to cut down the number of variations. This parameter, ($K_g = I + Ae^2$), can replace the girder inertia (I), girder area (A), and girder eccentricity (e). Bridge decks with the same K_g and different I, A, and e values are found not significantly affected the final distribution factors .

A similar analysis was conducted by Zokaie [3] for several models by keeping all the parameters as average value, except for one that varied from its minimum to its maximum. The same process was repeated for all parameters to determine the key parameters for each bridge type such as girder spacing (S), span length (L), girder stiffness (K_g), and slab thickness (t). Variation of truck axle width (gauge) was not considered because the design truck has a fixed gauge width. Most permitted trucks have a larger gauge width, which results in lower distribution factors. Therefore, using

simplified formulas that are developed based on the design truck will produce conservative results for permitted trucks .

According to the sensitivity studies conducted both in the NCHRP 12-26 Project; girder spacing (S) was the most sensitive parameter in determining the live load distribution factors (LLDF). Span length (L) is the next most sensitive parameter and longitudinal stiffness (Kg) has less of an effect on the LLDF and slab thickness (t) appears to be least sensitive in computing the LLDF.

As a result of the sensitivity studies, some parameters were kept such as girder spacing and span length since they have a significant effect on LLDF. And other parameters eliminated from the new simplified LLDF equations such as the slab thickness and the longitudinal stiffness [11]. The longitudinal stiffness parameter (Kg) was found to be associated to the span length parameter (L) since the general trend of the relationship is that Kg increases as L increases.

2.5 Current AASHTO Formulas for Box Girder Bridge.

The equations developed in NCHRP 12-26 needed to be modified to be consistent with the LRFD specifications. Live load description and multiple presence factors are the two issues of particular importance in comparing the live load response calculation procedures of the AASHTO 16th edition and LRFD specifications. The live load truck in the AASHTO 16th edition consists of either an HS20 truck or a lane load; whereas, the live load in the LRFD is combination of both a HS20 truck and a lane load. Both trucks have a 6 ft axle width, which is the most important factor affecting the transverse distribution of live loads. Therefore, it was assumed that the difference in the live load

configuration does not affect the live load distribution [3]. The formulas for different types of bridge superstructures such as concrete box girders, steel beam, and precast concrete I section needed to be revised to reflect this difference. For concrete box girder bridge, the first derivative of the distribution equation for interior and exterior girders (before the simplification) is shown in table 2.1 and 2.2.

Table 2.1: Formulas for Moment Distribution in Interior Girders

Bridge Type	Bridge Designed for One Traffic Lane	Bridge Designed for Two or More Traffic Lanes	Range of Applicability
Concrete Box Girders	$(3 + \frac{S}{2.2f}) (\frac{f}{L})^{0.35} (\frac{1}{N_c})^{0.45}$	$\frac{2.5}{N_c} - \frac{1}{N} + \frac{L}{800f} + (\frac{S}{9f})(\frac{90f}{L})^{0.25}$	$7f \leq S \leq 13f$ $60f \leq L \leq 240f$ $3 \leq N_c$

Table 2.2: Formulas for Moment Distribution in Exterior Girders

Bridge Type	Bridge Designed for One Traffic Lane	Bridge Designed for Two or More Traffic Lanes	Range of Applicability
Concrete Box Girders	$\frac{W_e}{7f}$	$\frac{W_e}{7f}$	$W_e \leq S$

Then, the formulas for concrete box girder were incorporated in to the LRFD specifications, table 2.3, after accurate distribution factors was calculated using the finite-element models, and then the formulas were refined to these results. Note that the formulas in table 2.3 are presented in a slightly different format than the LRFD

specifications (i.e., as wheel load distribution factors) to allow easier comparison. These formulas are based on unit less ratios of parameters [3].

Table 2.3: AASHTO-LRFD Formulas for Moment Distribution (g) in Interior Girders

Bridge Type	Bridge Designed for One Traffic Lane	Bridge Designed for Two or More Traffic Lanes	Range of Applicability
Concrete Box Girders	$(3 + \frac{S}{1.8f}) (\frac{f}{L})^{0.35} (\frac{1}{N_c})^{0.45}$	$2 (\frac{13}{N_c})^{0.3} + (\frac{S}{5.8f}) (\frac{f}{L})^{0.25}$	$7f \leq S \leq 13f$ $60f \leq L \leq 240f$ $3 \leq N_c$ if $N_c > 8$ use $N_c = 8$

Table 2.4 and 2.5 show the distribution formula cited in the current AASHTO LRFD for bridge type “d”, cast-in-place multi cell concrete box girders, were derived by first positioning the vehicle longitudinally, and then transversely, using an I-section of the box.

Table 2.4: Distribution of Live Load for Moment in Interior Girder, AASHTO LRFD

Bridge Type	Bridge Designed for One Traffic Lane	Bridge Designed for Two or More Traffic Lanes	Range of Applicability
Cast-in-Place Concrete Multi-Cell Box	$(1.75 + \frac{S}{3.6}) (\frac{1}{L})^{0.35} (\frac{1}{N_c})^{0.45}$	$(\frac{13}{N_c})^{0.3} (\frac{S}{5.8}) (\frac{1}{L})^{0.25}$	$7f \leq S \leq 13f$ $60f \leq L \leq 240f$ $3 \leq N_c$

Table 2.5: Distribution of Live Load for Moment in Exterior Girder, AASHTO LRFD

Bridge Type	Bridge Designed for One Traffic Lane	Bridge Designed for Two or More Traffic Lanes	Range of Applicability
Cast-in-Place Concrete Multi-Cell Box	$g = \frac{We}{14}$	$g = \frac{We}{14}$	$We \leq S$

In order to apply the LRFD Specifications [1] to a cast-in-place multi-cell box bridge, the bridge must have a constant width; parallel beams with approximately equal stiffness; span length of the superstructure exceeding 2.5 times the width, and a central angle up to 34 degrees. These restrictions became the objective of a study by Song et al. [10]. A detailed study was conducted to investigate whether or not these limits could be extended to include most of the box-girder bridge designs in California. In general, the analysis results from this study indicated that the current LRFD distribution factor formulae for concrete box-girder bridges provide a conservative estimate of the design bending moment and shear force. Also, the results show that the LRFD formulae are more conservative when estimating design forces in the exterior girders, especially for shear forces.

CHAPTER 3

DESCRIPTION OF MODEL BRIDGE AND LIVE LOADING

3.1 Selection of the Span Length for the Box Girder Bridge

In this study, different span lengths from support to support are used (80, 90, 100, 115, 120, 140) ft to study the effect of various span lengths on LLDF. These lengths lie within the typical length of precast concrete box girder bridges according to design aids published by the California Department of Transportation [13]. All straight and curved bridges that used are prismatic in cross section and continuous over the interior support. Figs 3.1-3.2 show the span length that considered for straight and curved bridges.

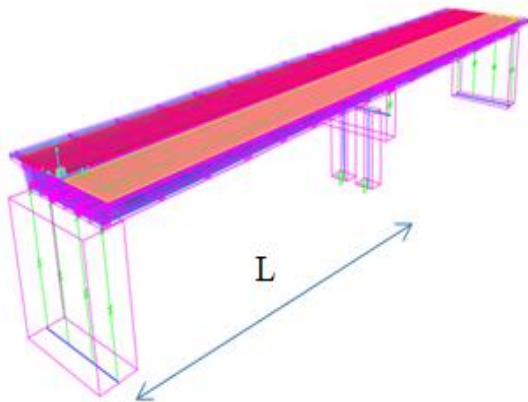


Figure 3.1: Span Length for Straight Bridge

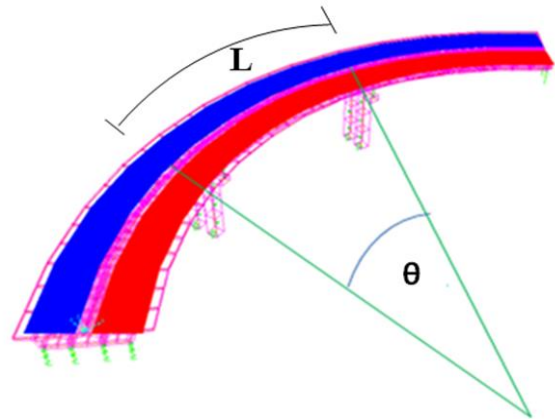


Figure 3.2: Span Length for Curved Bridge

3.2 Proposed Bridge Geometry

The geometry that used in this study based on real geometry from some bridges in Iraq, designed by a company, and constructed in different location in Iraq. The goal of using real geometry in this study is to obtain more realistic, accurate, and practical

results. Fig 3.3 shows the exact real geometry for span length of 115 ft for one of those bridges that have been designed and constructed in Samawah, Iraq. The all proposed geometry and properties for the bridge are following:

- Total deck width edge-to-edge, 32.5 feet that allows to have two design lanes,
- Total deck depth, 4.2-7.5 feet
- Use three-cell box girder
- Top slab thickness (t_1) = 0.8-1.2 ft., bottom slab thickness (t_2) = 1- 1.5 ft.
- Exterior Girder Thickness (t_3) = 1.3- 2 ft., Interior Girder Thickness (t_4) = 1- 1.35 ft.
- Left and right overhang outer length (t_5, t_6) = 0.7- 0.82 ft.
- Left and right overhang length (L_1, L_2) = 3.95ft
- Variable central angles from (38-60) degrees, and variable lengths from (80ft- 120 ft)
- Concrete Strength 576 Ksf (4Ksi)

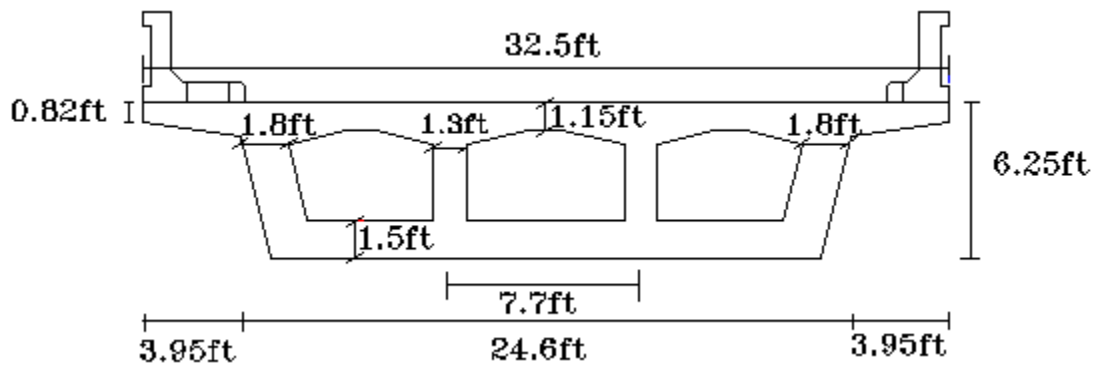


Figure 3.3: Real Geometry of the Box Girder for Span Length of 115 ft

For modeling and analyzing straight and curved bridges, some geometry are kept constant such as total deck width, number of cells (3 cells), left and right overhang, concrete strength and the girder spacing. The other geometry and properties, on the other hand, are different depending on the span length.

3.3 Description of Finite Element Models

3.3.1 Boundary Conditions of the Bridge Bearing

The point of placing the bearings between the bridge girders and their supports is to support the gravity loads (dead load and live loads) and accommodate the changes in the length of the bridge resulting from temperature variations and rotations that caused by bending. The bearings are usually designed to carry vertical loads and to accommodate horizontal movements of the bridge girders. Therefore, In this study, the boundary condition for the bridge bearing is fixed in vertical and out of plane directions and it is kept free in all other directions (rotations and translation along layout line) to represent the reality behavior of the bridge bearing. Also, the bearing is connected to girder bottom only (no integral situation).

3.3.2 Element Type of the Bridge

There are different numerical methods for analysis of box girders. The most efficient way to analyze box girders and obtain detailed results is through finite element modeling. The finite-element method using shell elements may be used for the box-girder bridge [14]. The shell element is a three or four-node area object used to model three-

dimensional structures. Shell objects are useful for simulating floor, wall, and bridge deck systems; 3-D curved surfaces; and components within structural members, such the web and flanges of a W-Section [12].

In this study, 3-D modeling analyses with shell element approach have been considered to model the concrete box-girder bridge as recommended by CSiBridge software program [12] and several researches [14]. Each shell element is a four-node area object used to model the entire bridge (superstructure and substructure). The superstructure and substructure of the box girder bridge is connected through link elements; each link has six degrees of freedom. The bottoms of these link elements connect the bent cap to joints at the bearing, while the tops of the links create bearing joints at the bottom of the superstructure. The properties assigned to these links simulate rigid connections. Spring supports are also used to model the connection of the bottom of the abutments with the ground (soil). Spring supports are link elements that are used to elastically connect joints to the ground with six degrees of freedom. All degrees of freedom of the spring supports are fixed to represent rigid restraints at the bottom of abutments.

3.4 Live Loading

3.4.1 Traffic Loads

In this study, the distribution factors were calculated using the AASHTO HL-93 design vehicular loads, AASHTO 2012. The HL-93 loads consist of a single design truck combined with a design lane load (Fig 3.4) Extreme load effects, as characterized by the largest positive and negative bending moments and shear forces, are determined using the

HL-93 load combinations per LRFD specifications AASHTO 2012. In addition, two trucks type HL-93 are used for the maximum negative bending moment, AASHTO 2012, (Fig 3.5). The magnitude of two truck load is reduced to 90% including that of the design lane load. For the design truck, the transverse spacing of the wheels is 6 feet, Fig (3.6).

To easily distinguish between the two types of trucks used for either positive or negative moment regions, the HL-93K is used to refer to a single design truck combined with a design lane load as shown in (Fig 3.4). Whereas, HL-93S is used to refer to two trucks combined with a design lane load as shown in (Fig 3.5). The HL-93S loading type consists of two design trucks that applied with a minimum headway between the front and rear axles of the two trucks equal to 50 feet, and it is considered for continues span bridges.

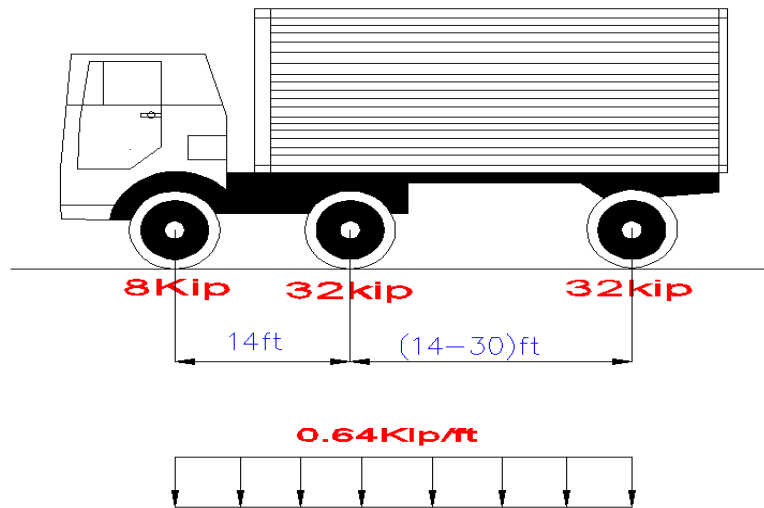


Figure 3.4: For the Maximum Positive Bending Moment Effect

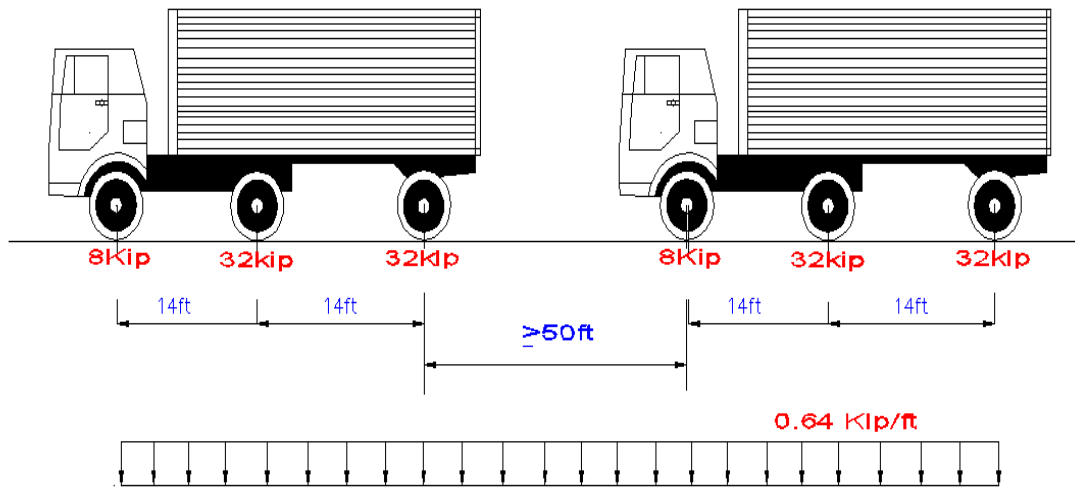


Figure 3.5: For the Largest Negative Moment Effects in Continues Span Bridges

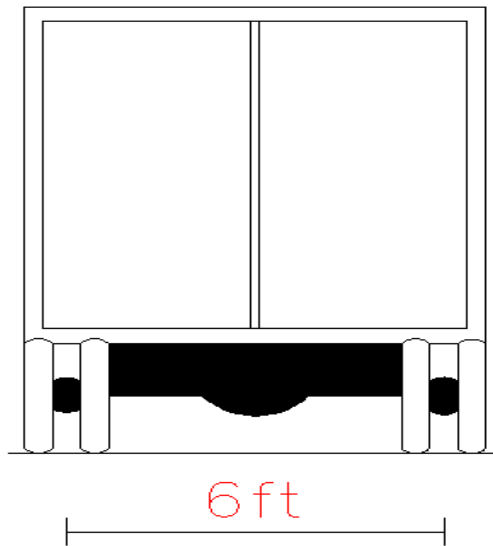


Figure 3.6: Spacing of the Wheels

3.5 One and Two Lane Moments

The maximum one or two lane moment is caused either by a single design lane or two (or more) design lanes. The analysis involves the determination of the load in one and two lanes and load distribution to girders. The effect of multiple design lanes is determined by superposition. The maximum effects are calculated as the largest of the following cases:

- (1) One lane fully loaded by a single truck and the other lane unloaded, Fig 3.7- 3.8
- (2) One lane fully loaded by two trucks and the other lane unloaded, Fig 3.7- 3.8
- (3) Both lanes loaded by a single truck, Fig 3.9
- (4) Both lanes loaded two trucks, Fig 3.9

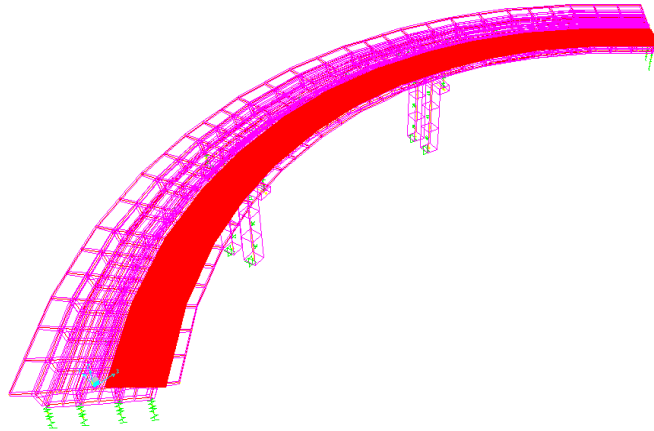


Figure 3.7: One Lane Fully Loaded and the Other Lane Unloaded, Right Lane

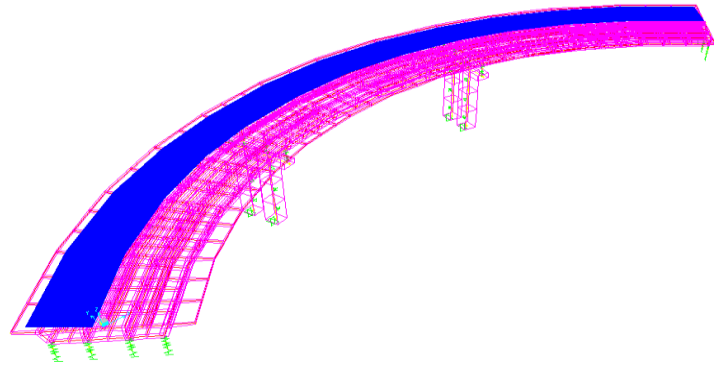


Figure 3.8: One Lane Fully Loaded and the Other Lane Unloaded, Left Lane

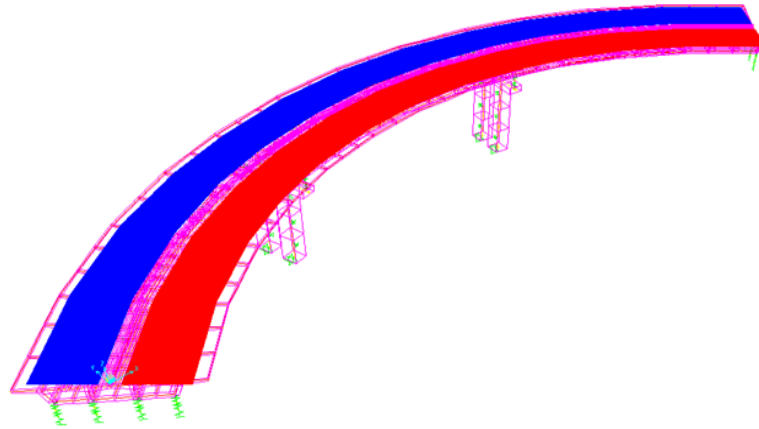


Figure 3.9: Both Lanes Loaded

For the all four cases mentioned, the distribution factors were calculated by loading the deck model with truck loads positioned at the longitudinal location that produces the maximum moment. The trucks were then moved transversely across the width of the bridge, and for each location the maximum girder moment was calculated, Figs 3.10. The largest girder (web) moment for all locations and load combinations was then selected as the maximum moment. This procedure was repeated for one and two number of design lanes that fit on the bridge transversely.

Then, the maximum moment was adjusted by the multiple presence reduction factors. The maximum moments that obtained from the analysis due to truck type HL-93K and HL-93S for each loading case were multiplied by these factors that depending on the number of lines as listed in table 3.1. The multiple presence reduction factors considered for possible combination of the number of loaded lanes, AASHTO, LRFD table 3.6.1.1.2-1.

After that, the controlling moment (greatest moment among all the maximum moments) was then selected to determine the live load distribution factors (LLDF). Formula 3.1 is used to calculate LLDF.

$$\text{LLDF} = M_{\text{max girder}} / M_{\text{max entire bridge}} \quad (\text{Formula 3.1})$$

Where: M_{girder} : Maximum moment on the girder for all load combination

$M_{\text{max entire bridge}}$: Maximum moment from a simple beam-line analysis of one lane of traffic

Table 3.1: Multiple Presence Factors

Number of Loaded Lanes	Multiple Presence Factors “m”
1	1.20
2	1.00
3	0.85
>3	0.65

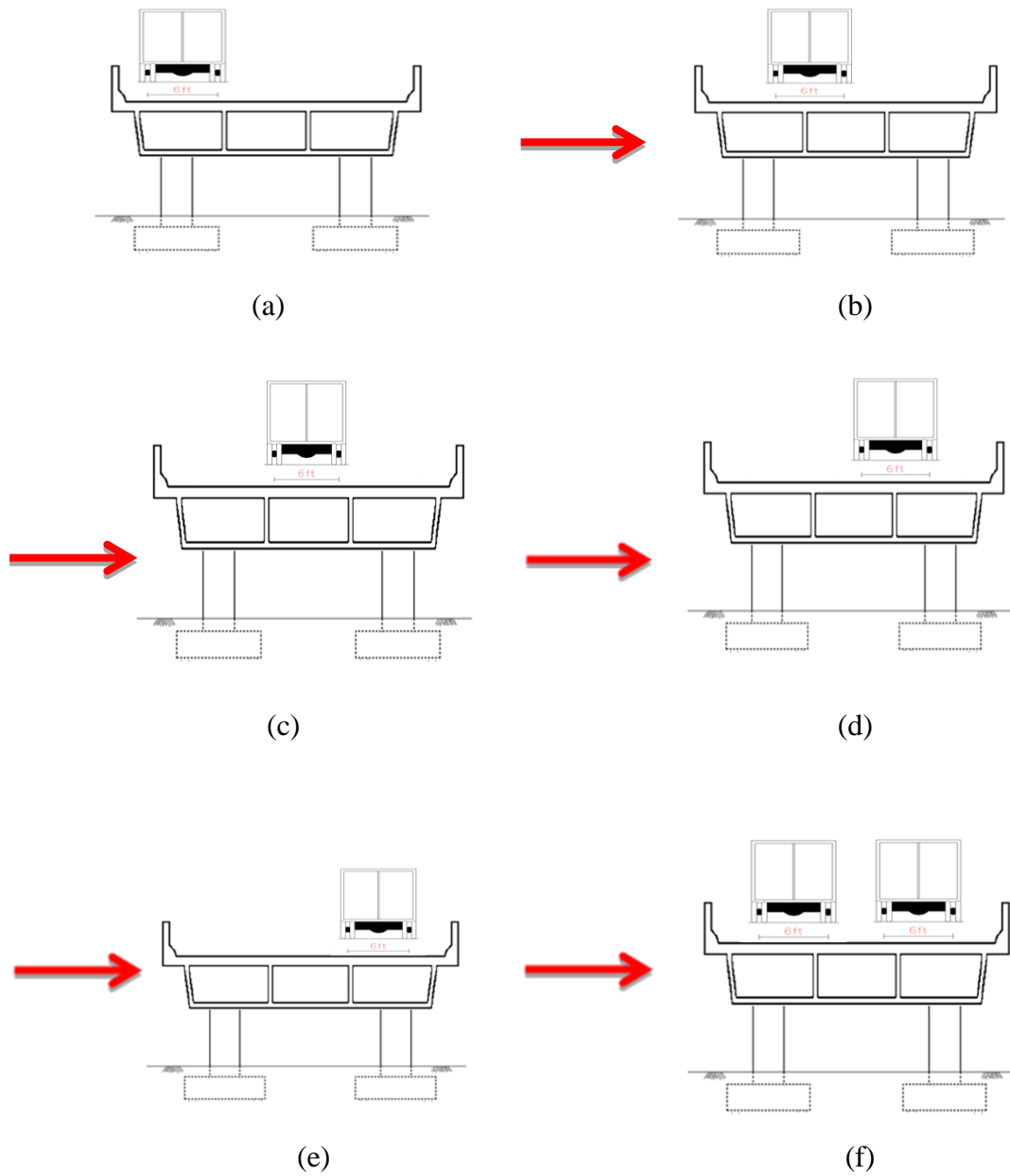


Figure 3.10: The transverse position of the trucks. (a), (b), (c), (d), and (e) Placing the trucks transversely across the width of the bridge (one lane loaded). (f) Two lanes loaded by the trucks that fit transversely on the bridge.

This procedure for determination of the live load distribution factors was repeated for the each span length that considered in this study (80, 90, 100, 115, 120, 140) ft.

Then, the results of the straight bridge analyses are discussed in the Chapter 4. The values of live distribution factors are tabulated and figures for negative and positive moment diagrams are provided. In addition, the results of live load distribution factors are plotted versus the span lengths and compared with those obtained from AASHTO LRFD formulas as explained in details Chapter 4.

CHAPTER 4

STRAIGHT BRIDGE MODEL AND ANALYZING

4.1 Modeling Straight Bridges

3-D modeling analyses have been conducted for straight bridges, Fig 4.1, for different span lengths (80, 90, 100, 115, 120, and 140 ft) and then the results compared with AASHTO LRFD, 2012 equations. This will help to get an indication and conception about the LLDF obtained from AASHTO LRFD formulas, 2012 to those obtained from finite element analyses for this type of bridge (Concrete Box Girder). Table 4.6.2.2.2b-1 and 4.6.2.2.2d-1, from AASHTO LRFD, 2012 [1] were used to calculate the LLDF for both interior and exterior girders, typical cross section (d) for Cast-in- Place Concrete Multi-cell Box, Fig 1.1. CSiBridge 2015, finite element analysis software program is being used to conduct 3-D modeling and the analyses as mentioned in details in Chapter 3.

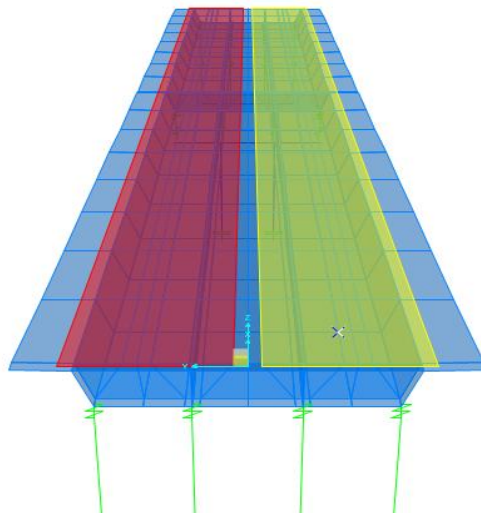


Figure 4.1: 3-D Modeling of the Bridge by Using CSiBridge Program (2015)

4.2 Results and Discussions for Straight Bridges

The analysis is conducted for different span lengths (80, 90, 100, 115, 120, 140 ft) to study the effect of different span lengths on LLDF and for different depths (4.1- 8.3 ft) that change along with span length. Also, other parameters like web thickness, top, and bottom slab thickness are considered to be variable with span length. No skew has been taken into account. For each length, the following six conditions are considered for straight bridges. The notations K and S are used for HL-93 design truck loads to distinguish between the two types of trucks as mentioned in section 3.4.1.

1. Left design lane loaded only by one truck (HL-93K)
1. Right design lane loaded only by one truck (HL-93K)
2. Two design lanes loaded by one truck (HL-93K)
3. Left design lane loaded only by two trucks (HL-93S)
4. Right design lane loaded only by two trucks (HL-93S)
5. Two design lanes loaded by two trucks (HL-93S)

The values of the load distribution factors are obtained in all of the above cases for each interior and exterior girder at their critical locations corresponding to the maximum positive and negative bending moments. Fig 4.2 shows the moment diagram and the results of maximum negative and positive moments due to truck HL-93K. The moment diagram and the result of negative moment only due to truck HL-93S is shown in Fig 4.3. These moment diagrams and the results observed in Figs 4.2-4.3 are for the case of two lanes loaded, the moment result of entire bridge, and for span length of 80 feet. The results of moments for all other cases are attached in the Appendix A.

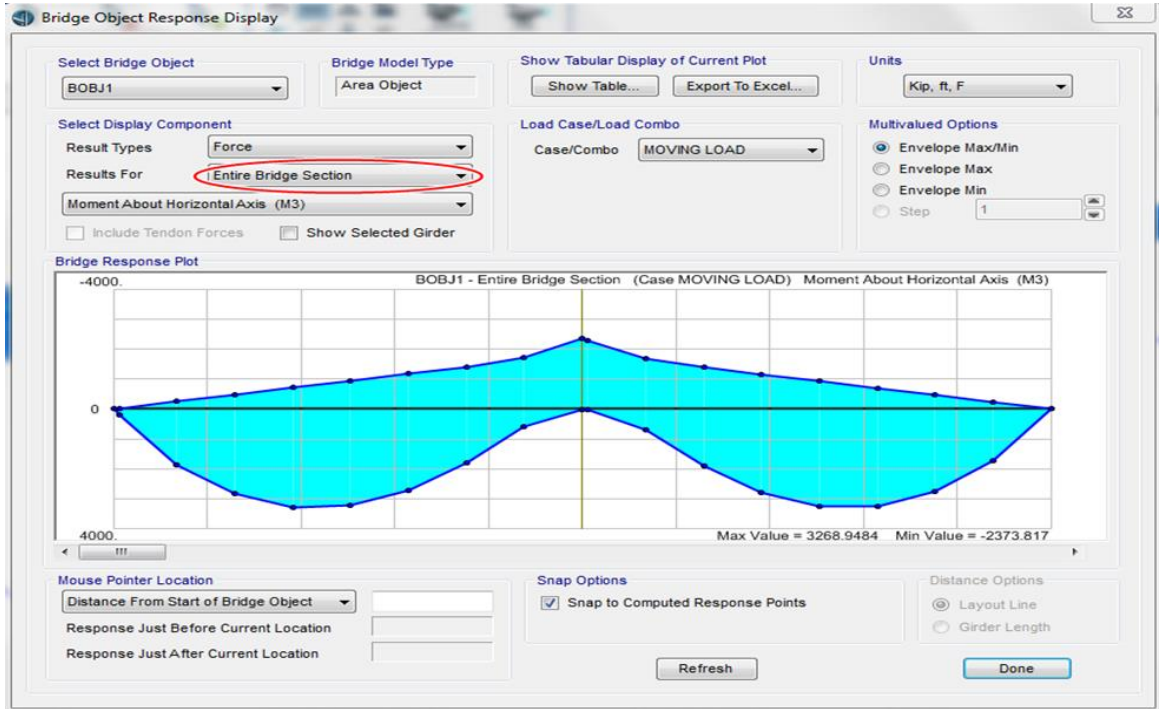


Figure 4.2: Entire Bridge (80 ft, Two Lanes Loaded)

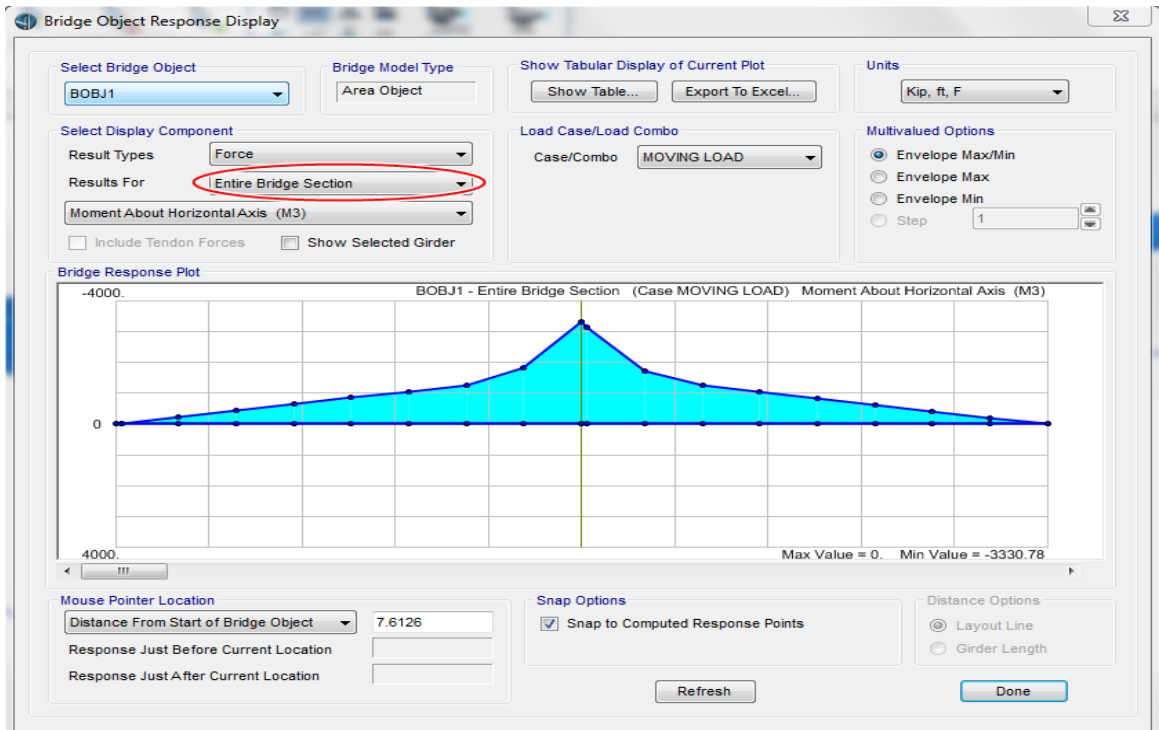


Figure 4.3 Entire Bridge (80 ft, Two Lanes Loaded)

4.2.1 Negative Moment (HL-93S)

Dual trucks combined with design lane load are used to determine live load distribution factors (LLDF) for the maximum negative bending moment. Table 4.1 shows the LLDF for one lane loaded by two trucks (HL-93S). Using an 80 ft span length as an example, the maximum LLDF for interior girder is 0.33, while the LLDF calculated from AASHTO LRFD is 0.51, Fig 4.4. The difference between the two is about 35%. With the truck loaded on the right lane, the maximum LLDF for exterior girders accrued on the right girder with a difference of about 35% as observed in Fig 4.5. The same value of the maximum distribution factor was obtained when left lane was loaded, but occurred on the left girder that is closest to the truck load. Table 4.2 shows the LLDF for two lanes loaded. The results indicate that the percentage difference between AASHTO LRFD formula and finite element analysis is about 16% for span length of 80ft and 13.3% for span length of 140 ft as shown in Fig 4.6.

4.2.2 Positive and Negative Moments (HL-93K)

A single design truck combined with a design line load is typically used to determine the maximum positive moments. The back to back truck placement with 50 ft spacing (HL-93S in this thesis) normally controls for negative moment regions in bridges with long spans as those being studied in this research. However, a single truck must also be checked to see if it governs design of negative moment regions. First, the LLDF is determined for one lane loaded due to maximum positive and negative moments effect, Table 4.3 and 4.4. Then the LLDF is calculated for two lanes loaded under the maximum positive and negative moments as shown in table 4.5 and 4.6.

4.2.2.1 Maximum Positive Moment

For positive one lane loaded the results show that the LLDFs calculated from AASHTO LRFD are 39-40 % greater than those obtained from an analysis of interior girders, Fig 4.7 and 44% as an average for exterior girders, Fig 4.8. For the case of two designs lane loaded, the AASHTO LRFD formula gave about a 16% greater bending moment than those determined from the analysis for interior girders as observed in Fig 4.11 and about 20% for exterior girders.

4.2.2.2 Maximum Negative Moment

Table 4.4 shows the results of LLDF for the negative bending moment in both exterior and interior girders for a one design lane loaded case. About 35% is the percentage difference between the LLDF results that obtained from the analysis and AASHTO LRFD formula for interior girder, Fig 4.9 and about 37.5% in exterior girders as shown in Fig 4.10. For two lanes loaded, the percentage difference is 14% for interior girders, Fig 4.12. With that lowest difference among the other load cases, the LLDF for the maximum negative bending moment for a single truck load (HL-93K) represents the largest bending moment of the all loading cases as shown in table 4.6.

According to the AASHTO LRFD, 4.6.2.2.1 [1] and WSDOT BDM [13], the entire slab width shall be assumed effective for compression. It's both economical and desirable to design the entire superstructure as a unit slab rather than as individual girders. That is by multiplied the LLDF for interior girders by the number of webs to obtain the design live load for the entire superstructure. Therefore, the results of LLDF for interior girders that determined from AAHTO LRFD and finite element analysis were multiplied by four,

which is the total number of webs on the box girder bridge used in this study. Table 4.7 and Fig 4.13 show the maximum LLDF for entire girders (bridge).

4.3 Live Load Distribution Factors (LLDF) for Straight Bridges

Tables 4.1 – 4.6 show LLDF for all cases of loading. The bold numbers in the columns represent the maximum moments for interior and exterior girders, for each span length.

Table 4.1: LLDF for Negative Moment Due to HL-93S- One Lane Loaded

Span Length (ft)	Interior Girder 1	AASHTO LRFD	Interior Girder 2	AASHTO LRFD	Left Exterior Girder	AASHTO LRFD	Right Exterior Girder	AASHTO LRFD
80	0.30	0.51	0.33	0.51	0.16	0.46	0.30	0.45
90	0.29	0.49	0.32	0.49	0.17	0.45	0.29	0.45
100	0.28	0.47	0.31	0.47	0.18	0.45	0.29	0.45
115	0.26	0.45	0.3	0.45	0.19	0.45	0.28	0.45
120	0.26	0.44	0.29	0.44	0.2	0.44	0.28	0.44
140	0.25	0.42	0.28	0.42	0.21	0.44	0.27	0.43

Table 4.2: LLDF for Negative Moment Due to HL-93S- Two Lanes Loaded

Span Length (ft)	Interior Girder 1	AASHTO LRFD	Interior Girder 2	AASHTO LRFD	Left Exterior Girder	AASHTO LRFD	Right Exterior Girder	AASHTO LRFD
80	0.58	0.69	0.58	0.69	0.42	0.56	0.42	0.56
90	0.57	0.67	0.57	0.67	0.45	0.55	0.45	0.55
100	0.56	0.65	0.56	0.65	0.46	0.55	0.46	0.55
115	0.55	0.63	0.55	0.63	0.47	0.55	0.47	0.55
120	0.54	0.62	0.54	0.62	0.47	0.54	0.47	0.54
140	0.52	0.60	0.52	0.60	0.48	0.54	0.48	0.54

Table 4.3: LLDF for Positive Moment Due to HL-93K- One Lane Loaded

Span Length (ft)	Interior Girder 1	AASHTO LRFD	Interior Girder 2	AASHTO LRFD	Left Exterior Girder	AASHTO LRFD	Right Exterior Girder	AASHTO LRFD
80	0.27	0.51	0.31	0.51	0.19	0.48	0.27	0.48
90	0.27	0.49	0.3	0.49	0.19	0.47	0.26	0.47
100	0.26	0.47	0.29	0.47	0.2	0.46	0.25	0.46
115	0.25	0.45	0.28	0.45	0.21	0.45	0.24	0.45
120	0.25	0.44	0.27	0.44	0.21	0.45	0.24	0.45
140	0.24	0.42	0.25	0.42	0.22	0.44	0.23	0.43

Table 4.4: LLDF for Negative Moment Due to HL-93K- One Lane Loaded

Span Length (ft)	Interior Girder 1	AASHTO LRFD	Interior Girder 2	AASHTO LRFD	Left Exterior Girder	AASHTO LRFD	Right Exterior Girder	AASHTO LRFD
80	0.29	0.51	0.33	0.51	0.16	0.48	0.3	0.48
90	0.28	0.49	0.32	0.49	0.17	0.47	0.29	0.47
100	0.28	0.47	0.31	0.47	0.18	0.46	0.29	0.46
115	0.26	0.45	0.3	0.45	0.19	0.45	0.28	0.45
120	0.26	0.44	0.29	0.44	0.19	0.44	0.28	0.45
140	0.25	0.42	0.27	0.42	0.20	0.44	0.28	0.43

Table 4.5: LLDF for Positive Moment Due to HL-93K- Two Lanes Loaded

Span Length (ft)	Interior Girder 1	AASHTO LRFD	Interior Girder 2	AASHTO LRFD	Left Exterior Girder	AASHTO LRFD	Right Exterior Girder	AASHTO LRFD
80	0.58	0.69	0.58	0.69	0.44	0.55	0.44	0.55
90	0.57	0.67	0.57	0.67	0.44	0.55	0.44	0.55
100	0.56	0.65	0.56	0.65	0.45	0.55	0.45	0.55
115	0.54	0.63	0.54	0.63	0.45	0.55	0.45	0.55
120	0.53	0.62	0.53	0.62	0.46	0.54	0.46	0.54
140	0.50	0.60	0.50	0.60	0.47	0.53	0.47	0.53

Table 4.6: LLDF for Negative Moment Due to HL-93K- Two Lanes Loaded

Span Length (ft)	Interior Girder 1	AASHTO LRFD	Interior Girder 2	AASHTO LRFD	Left Exterior Girder	AASHTO LRFD	Right Exterior Girder	AASHTO LRFD
80	0.59	0.69	0.59	0.69	0.46	0.55	0.46	0.55
90	0.58	0.67	0.58	0.67	0.46	0.55	0.46	0.55
100	0.57	0.65	0.57	0.65	0.46	0.55	0.46	0.55
115	0.56	0.63	0.56	0.63	0.46	0.55	0.46	0.55
120	0.55	0.62	0.55	0.62	0.47	0.54	0.47	0.54
140	0.52	0.60	0.52	0.60	0.47	0.53	0.47	0.53

According to the analyses, the negative effect of HL-93K loading for two lanes loaded gives the largest maximum moments on both interior and exterior girders. The bold numbers present the greatest maximum moments.

4.4 Comparison of the Results for Straight Bridges

The comparison between LLDF obtained from AASHTO LRFD, 2012 [1] to those obtained from finite element analyses are shown in Figures 4.4–4.6 for HL-93S and in Figs 4.7-4.12 for HL-93K loading type.

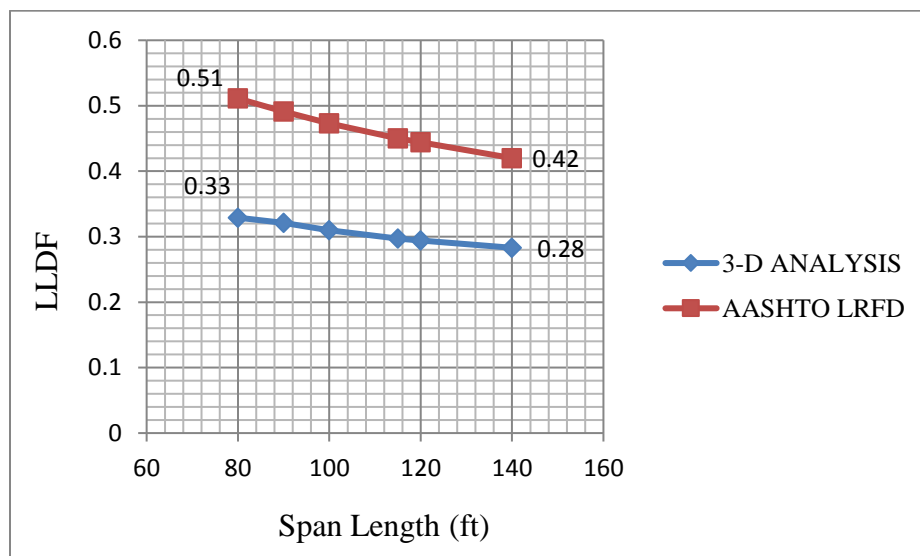


Figure 4.4: HL-93S- One Lane Loaded- Interior Girder

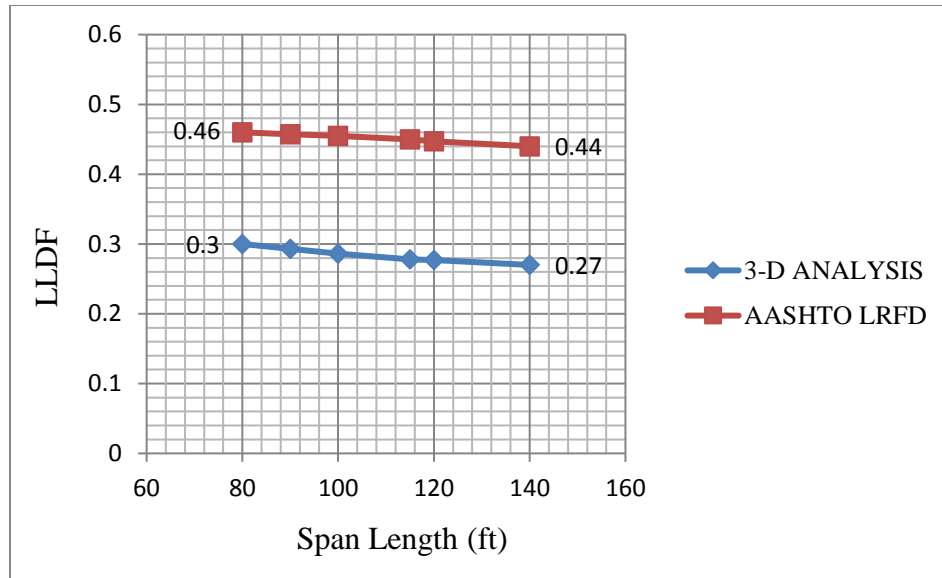


Figure 4.5: HL-93S- One Lane Loaded- Exterior Girder

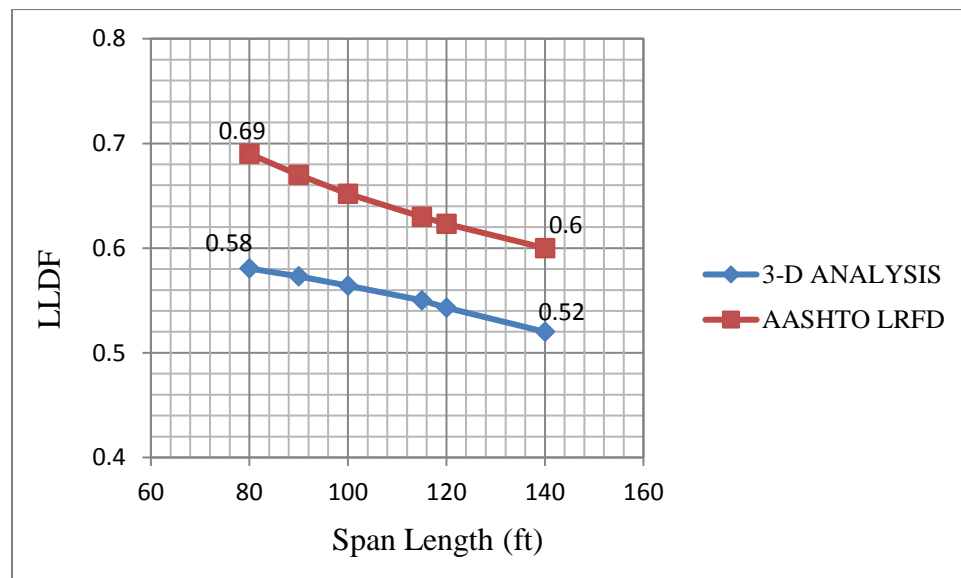


Figure 4.6: HL-93S- Two Lanes Loaded- Interior Girder

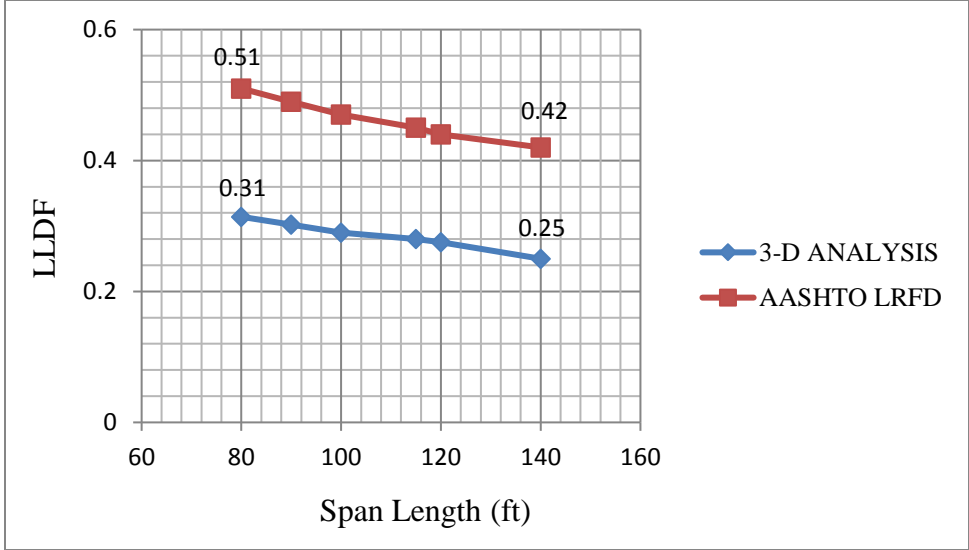


Figure 4.7: HL-93K- One Lane Loaded- Interior Girder (Positive Moment)

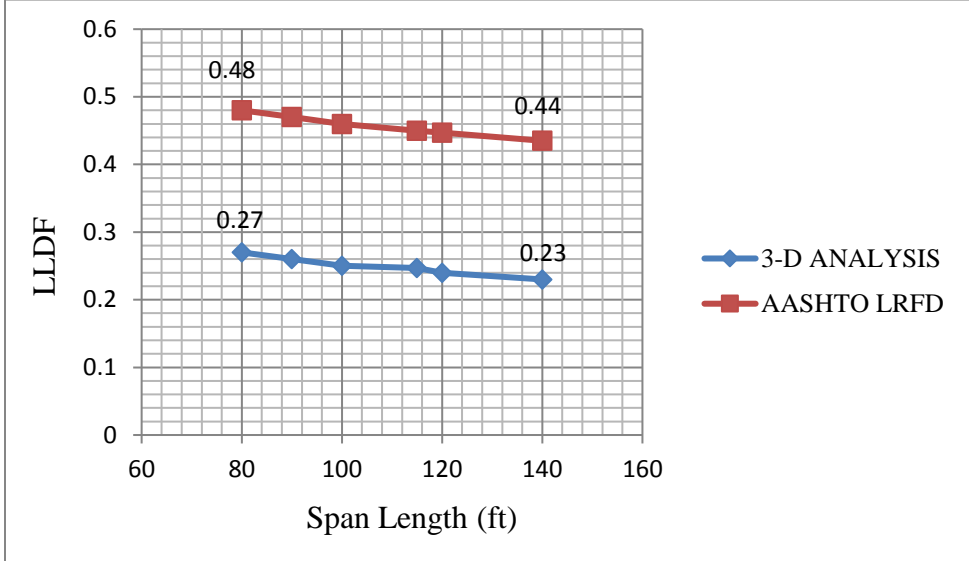


Figure 4.8: HL-93K- One Lane Loaded- Exterior Girder (Positive Moment)

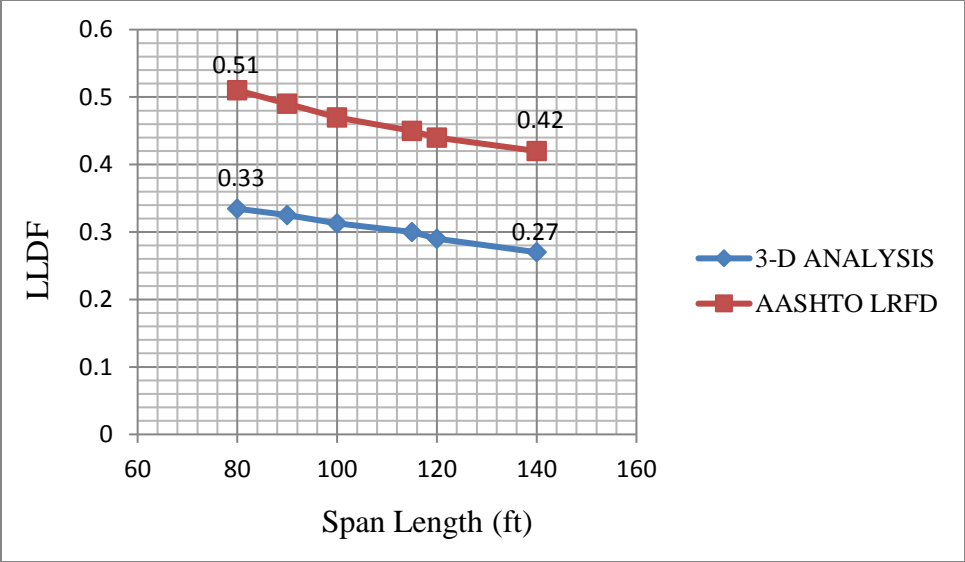


Figure 4.9: HL-93K- One Lane Loaded- Interior Girder (Negative Moment)

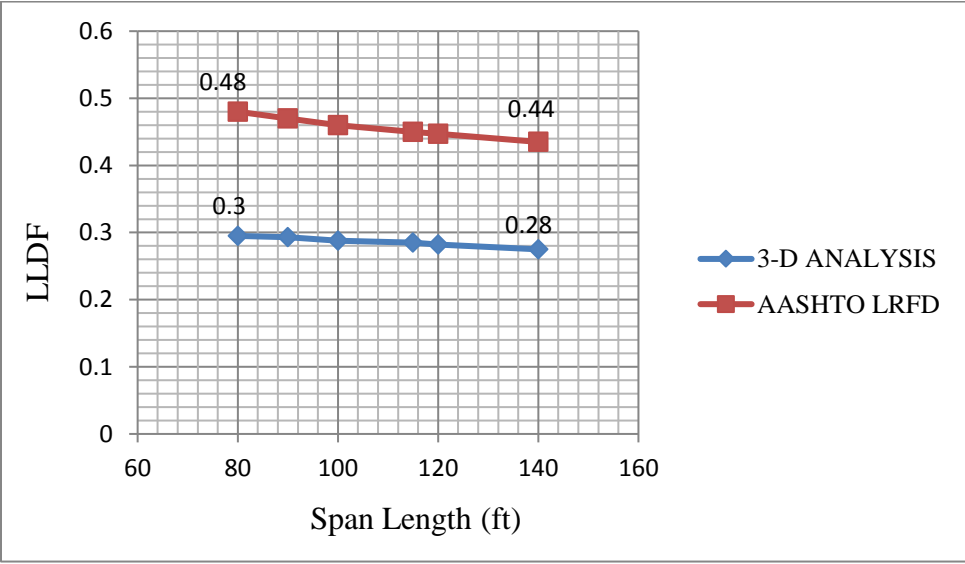


Figure 4.10: HL-93K- One Lane Loaded- Exterior Girder (Negative Moment)

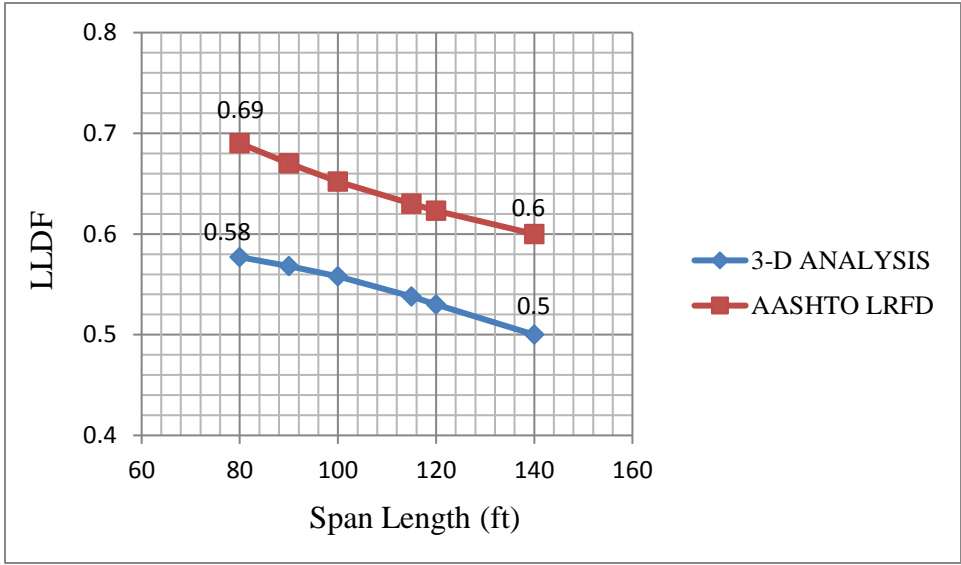


Figure 4.11: HL-93K- Two Lanes Loaded- Interior Girder (Positive Moment)

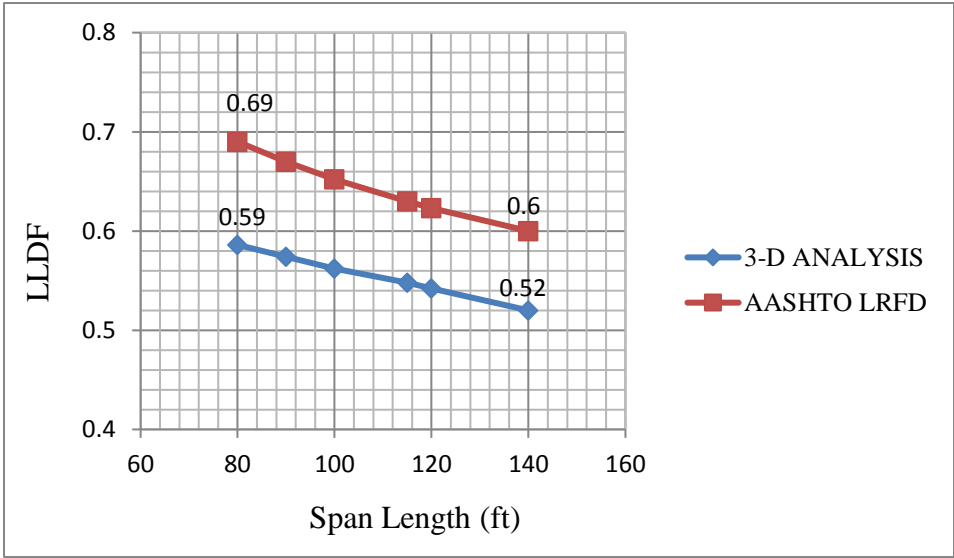


Figure 4.12: HL-93K- Two Lanes Loaded- Interior Girder (Negative Moment)

4.5 Distribution Factor for Entire Bridge

It's both economical and desirable to design the entire superstructure as a unit slab rather than individual girders as mentioned in section 4.2.4. That is by multiplied the LLDF for interior webs by the number of webs to obtain the design live load for the entire superstructure, Formula 4.1. Therefore, the results of LLDF for interior girders that determined from AAHTO LRFD and finite element analysis were multiplied by four (4), and the results are tabled and plotted for different span lengths as shown in table 4.7 and Fig 4.13.

$$DF = Nb * Dfi \quad \text{(Formula 4.1)}$$

Where: DF: Live load distribution factor for entire superstructure bridge

Dfi: Live load distribution factor for interior web

Nb: Number of webs

Table 4.7: Maximum LLDF for Entire Bridge

Straight Bridge					
Max LLDF on Individual Girder			Max LLDF on Entire Bridge		
Span Length (ft)	Interior Girder (Analysis)	AASHTO LRFD	Number of Webs	Interior Girder (Analysis)	AASHTO LRFD
80	0.59	0.69	4	2.36	2.76
90	0.58	0.67	4	2.32	2.70
100	0.57	0.65	4	2.28	2.61
115	0.56	0.63	4	2.24	2.52
120	0.55	0.62	4	2.20	2.50
140	0.52	0.60	4	2.08	2.40

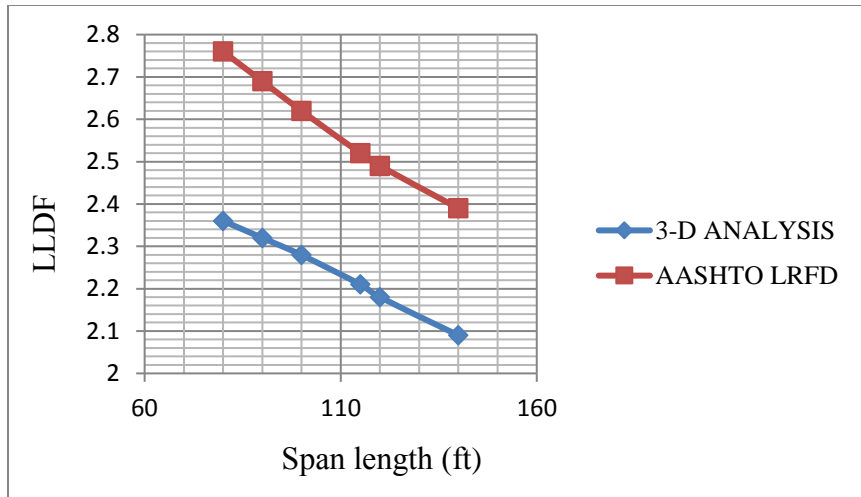


Figure 4.13: Maximum LLDF for the Entire Bridge

AASHTO LRFD provides formulas to determine live load distribution factors for several common bridge superstructure types. However, there is a restriction of using these equations for curved bridges having central angles that exceed 34 degrees. Chapter 5 provides a study and modeling analyses for horizontally curved concrete box girder bridges that have a degree of curvature greater than 34 degrees. Additionally, analyses were conducted for curved bridges that took into account the effect of centrifugal and braking forces as explained in the Chapter 5.

CHAPTER 5

CURVED BRIDGE MODELING AND ANALYSES

5.1 Curved Bridge Restrictions in AASHTO LRFD

Curved structures are often required for highway bridges, especially when separations or on-off ramps are involved. In the current LRFD specifications AASHTO 2012 there is a limit on using the distribution factor formula for curved bridges. More specifically, refined analyses are required for bridges with central angles greater than 34° in any one span from support to sport. This limit is rather restrictive, as geometric design often necessitates the construction of highly curved structures that exceed this limit [15].

5.2 Description of the Centrifugal Force, CE

When a truck is moving on a curved bridge, centrifugal force and track should be taken into account, Fig 5.1. For the purpose of determining the radial force or the overturning effect on wheel loads, the centrifugal effect on live load shall be taken as the product of the axle weights of the design truck and the factor C , According to AASHTO LRFD, 2012 taken as shown in Formula 5.1.

$$C = f v^2 / gR$$

(Formula 5.1)

Where: $f = 4/3$ for load combinations

$v =$ highway design speed (ft/s²)

$g =$ gravitational acceleration (32.2 ft/s²)

$R =$ radius of curvature of traffic lane (ft)

In this study, 20-40 mph is used as the highway design speeds (v) for curved bridges that are varies depending on the radius of curvature (R) according to the current edition of the AASHTO publication, A Policy of Geometric Design of Highways and Streets in 2001 [23]. The radius of curvature of traffic lane is determined using formula 5.2.

$$R = 360 L / 2\pi \theta \quad \text{(Formula 5.2)}$$

Where: L : span length of the bridge from support to support

θ : central angle between one span length

Centrifugal forces shall be applied horizontally at a distance 6.0 ft above the roadway surface, Fig 5.2. A load path to carry the radial force to the substructure shall be provided. The effect of super elevation in reducing the overturning effect of centrifugal force on vertical wheel loads is considered as 8% as recommended by A Policy of Geometric Design of Highways and Streets in 2001 [23].

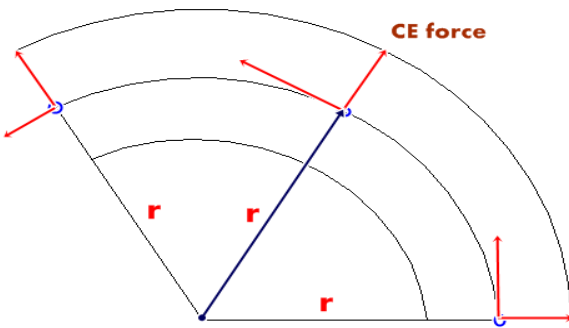


Figure 5.1: CE Force on Curved Bridge

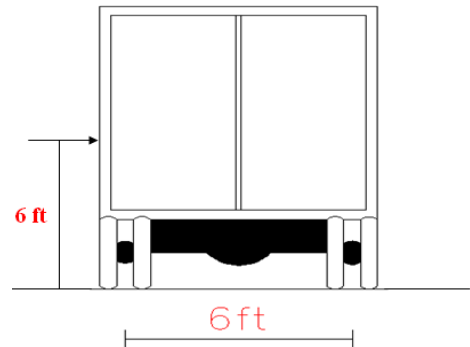


Figure 5.2: Distance of Centrifugal Force

Centrifugal force also causes an overturning effect on the wheel loads because the radial force is applied 6.0 ft above the top of the deck. Thus, centrifugal force tends to cause an increase in the vertical wheel loads toward the outside of the bridge and an

unloading of the wheel loads toward the inside of the bridge. Super elevation helps to balance the overturning effect due to the centrifugal force and this beneficial effect may be considered. Moreover, Centrifugal force is not required to be applied to the design lane load, as the spacing of vehicles at high speed is assumed to be large, resulting in a low density of vehicles following and/or preceding the design truck [1].

5.3 Braking Force, BR

The braking force shall be taken as the greatest of 25 percent of the axle weights of the design truck or five percent (5%) of the design truck plus lane load [1]. This braking force shall be placed in all design lanes which are considered to be loaded in accordance with Article 3.6.1.1.1 and which is carrying traffic headed in the same direction. These forces shall be assumed to act horizontally at a distance of 6.0 ft above the road way surface in either longitudinal direction to cause extreme force effects, Fig 5.3. All design lanes shall be simultaneously loaded for bridges likely to become one-directional in the future. The multiple presence factors specified in Article 3.6.1.1.2 shall apply.

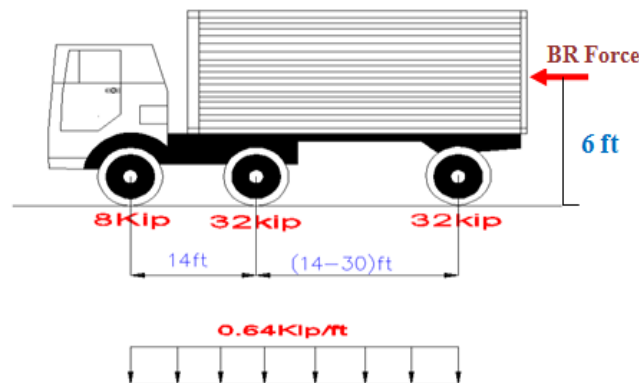


Figure 5.3: Truck Loads Plus Braking Force

5.4 Curved Bridge Modeling and Analysis

3-D modeling analyses are used to determine the LLDF for horizontally curved concrete box girder bridges that have central angles out of the LRFD specification. The 3-D modeling analyses have been conducted for the various span lengths that had already been used for straight bridges (80, 90, 100, 115, 120, and 140 ft) with different central angles (5° , 38° , 45° , 50° , 55° , and 60°). First, 3-D modeling analyses for different span lengths were conducted, while the central angles and other parameters remain constant. Next, finite element analysis modelings were conducted for different central angles, while the span length and other parameters remain constant. With that, the results of curved analyses can be compared with those obtained from AASHTO LRFD for straight bridges. Fig 5.4 and 5.5 show the curved bridges that have central angles greater than 34° .

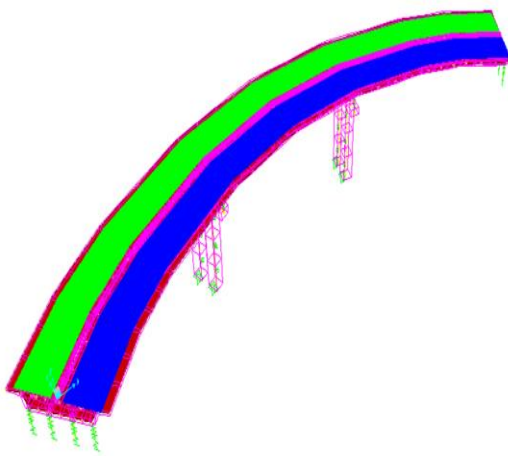


Figure 5.4: Curved Bridges with $\theta > 34^\circ$

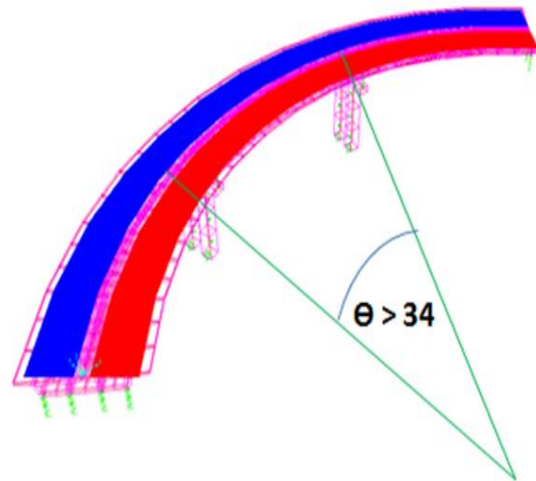


Figure 5.5: Curved Bridges with $\theta > 34^\circ$

5.5 Results and Discussion for Curved Bridges

5.5.1 Effect of the Curvature

According to AASHTO LRFD [1], the LLDF for straight bridges can be used for curved bridges that have central angles up to 34° . The goal of this study is to determine the LLDF with angles between bents exceeding that limit (34°), using 3-D finite element analysis. However, some modelings have been conducted for different span lengths of curved bridges with a 5° central angle, which is within the limits of the LRFD specification. The goal is to find out what the effect is of increasing the curvature of box girders from zero (straight bridge) to a small curvature with a central angle of 5° .

The LLDFs are determined by using a central angle of 38° , that is a little beyond the specification limits. After that, the angles between bents are increased to 45, 50, 55, and 60. For each central angle, the LLDFs are calculated for different span lengths (80, 90, 100, 115, 120, and 140). Then, the results of LLDF versus span lengths were plotted for: curved bridges with various central angles; straight bridges obtained from the analyses; and for straight bridges determined from AASHTO LRDF formulas. This was done to make it easier to compare and evaluate the results of LLDF for each case.

Truck type HL- 93K and HL-93S are used with a 5° angle of curvature to determine what the maximum bending moment is from these types of loading. The results of LLDF for curved bridges show that there is a slight difference between the LLDF that is obtained from analyses for straight bridges and the one that has a central angle of 5° as shown in table 5.1- 5.6 and Figs 5.6 - 5.8. Also, the maximum negative bending moment determined from two lanes loaded (truck type HL-93K), gives the greatest bending moment among the all of the previously mentioned six cases. Therefore, the analyses for the other central angles (38° , 45° , 50° , 55° , and 60°) are conducted using the negative

bending moment caused by the HL-93K truck load, since it gives the greatest moment that is used to calculate the LLDF.

Fig 5.9 and table 5.7 show the determination of LLDF for different span lengths, while the central angle of 38° remains constant. The results indicate that the LLDF's values are a bit greater than those obtained from AASHTO LRFD formulas for straight bridges. The values determined from LRFD formulas are conservative by about 3%. Even though there is no significant difference between the values, AASHTO's equations no longer can be used to determine LLDF for bridges having a central angle exceed 38° .

With a 45° angle of curvature, the percentage difference increases to about 6% as observed in table 5.8, and Fig 5.10. And, a 7.5% percentage difference between the LLDF obtained from AASHTO formulas and those determined using finite element analysis with a central angle of 50° , are shown in table 5.9 and Fig 5.11. In the same manner, the differences are 10%, 14.5% for the central angles of 55° and 60° . Tables 5.10, 5.11 and Figs 5.12, 5.13 show these differences. The results of greatest maximum moments for different span lengths and central angles are attached in Appendix A.

5.5.2 Effect of Centrifugal and Braking Forces

Due to the centrifugal (CE) force, . the maximum bending moment occurs on exterior girders, whereas the interior girders carry the minimum moment. Interior girders, however, are not designed with less capacity than exterior ones. Also, the bending moment generally increases under the braking force.

The finite element analysis has been conducted for curved bridges that have central angles outside the LRFD limits (34°) by including the effect of centrifugal and braking forces. The analyses are conducted for the same span lengths and central angles that had already used to determine LLDF for straight and curved bridges and with different central angles (38° , 45° , 50° , 55° , 60°). Truck HL-93K for two lanes loaded is used since this type of loading gives the greatest moment as pointed out before.

The results of these analyses are shown in tables 5.17-5.21 and Figs 5.14-5.18. To make it easier to compare and evaluate the results of LLDF for each case, the results of LLDF versus span lengths were plotted for: straight bridges obtained from the analyses; straight bridges determined from AASHTO LRDF formulas; curved bridges with various central angles. The results for curved bridges with various central angles show the effects of CE and BR and are also plotted in the same graphs. Even though these results with the effect of CE and BR are not direct LLDF since the LLDF is counted for vertical loads only, it would be useful to study the effects of moments due to CE and BR. All the results of LLDF are plotted for interior girders that carry the maximum loads. However, for curved bridges having the effect of CE and BR, the results are plotted for exterior girders since the maximum moment occurs on those due to the effects of CE and BR.

These values clearly indicate that the moments for exterior girders significantly increase due to the effects of centrifugal and braking forces. The increase in maximum moments for exterior girders even exceed the values of moments for interior girders for straight bridges that are usually supposed to have higher moment. For instance, the indirect distribution factor for a span length of 80 ft with a central angle of 38° is 0.89, whereas it is 0.46 for straight bridges, determined from LRDF formulas. This apparently

states that there is a big change in the indirect LLDF results for curved bridges due to the effects of CE and BR.

Tables 5.12 to 5.16 show the indirect distribution factors for entire bridge (all girders). The entire superstructure is designed as a unit slab rather than as individual girders as recommended by AASHTO LRFD, 4.6.2.2.1 [1] and WSDOT BDM [13]. All factors are multiplied by the number of girders (4) to take into account the LLDF for all interior and exterior girders.

5.6 Distribution Factor Results (LLDF) for Central Angle of 5°

Tables 5.1-5.6 show the LLDF on curved bridges using HL-93K and HL-93S truck loading on one and two traffic lanes separately with a central angle equal to 5°. These tables state the LLDF for interior girders that usually carry larger moments than those on exterior girders.

Table 5.1: LLDF for HL-93S- One Lane Loaded-Negative Moment

Span Length (ft)	Max Moment Interior Girder 2	AASHTO LRFD
80	0.33	0.51
90	0.32	0.49
100	0.31	0.47
115	0.30	0.45
120	0.29	0.44

Table 5.2: LLDF for HL-93S- Two Lanes Loaded-Negative Moment

Span Length (ft)	Max Moment Interior Girder 1	AASHTO LRFD
80	0.59	0.69
90	0.58	0.67
100	0.57	0.65
115	0.56	0.63
120	0.55	0.62

Table 5.3: LLDF for HL-93K- One Lane Loaded-Positive Moment

Span Length (ft)	Max Moment Interior Girder 2	AASHTO LRFD
80	0.33	0.51
90	0.32	0.49
100	0.31	0.47
115	0.29	0.45
120	0.28	0.44

Table 5.4: LLDF for HL-93K- One Lane Loaded-Negative Moment

Span Length (ft)	Max Moment Interior Girder 2	AASHTO LRFD
80	0.33	0.51
90	0.32	0.49
100	0.31	0.47
115	0.30	0.45
120	0.29	0.44

Table 5.5: LLDF for HL-93K- Two Lanes Loaded-Positive Moment

Span Length (ft)	Max Moment Interior Girder 2	AASHTO LRFD
80	0.59	0.69
90	0.58	0.67
100	0.57	0.65
115	0.56	0.63
120	0.55	0.62

Table 5.6: LLDF for HL-93K- Two Lanes Loaded-Negative Moment

Span Length (ft)	Max Moment Interior Girder 1	AASHTO LRFD
80	0.60	0.69
90	0.59	0.67
100	0.58	0.65
115	0.57	0.63
120	0.56	0.62

According to the analyses that were done for horizontally curved bridges, the negative effect of HL-93K loading for two lanes loaded gives the largest maximum moments on both interior and exterior girders.

5.7 Comparison of Results for Central Angle of 5°

Figures 5.6 shows the comparison of results that obtained from finite element analyses for HL-93S between LLDF for straight bridges and LLDF for curved bridges with a central angles of 5°. Fig 5.7-5.8 show the comparison for HL-93K loading type. The results that determined from AASHTO LRFD are also plotted.

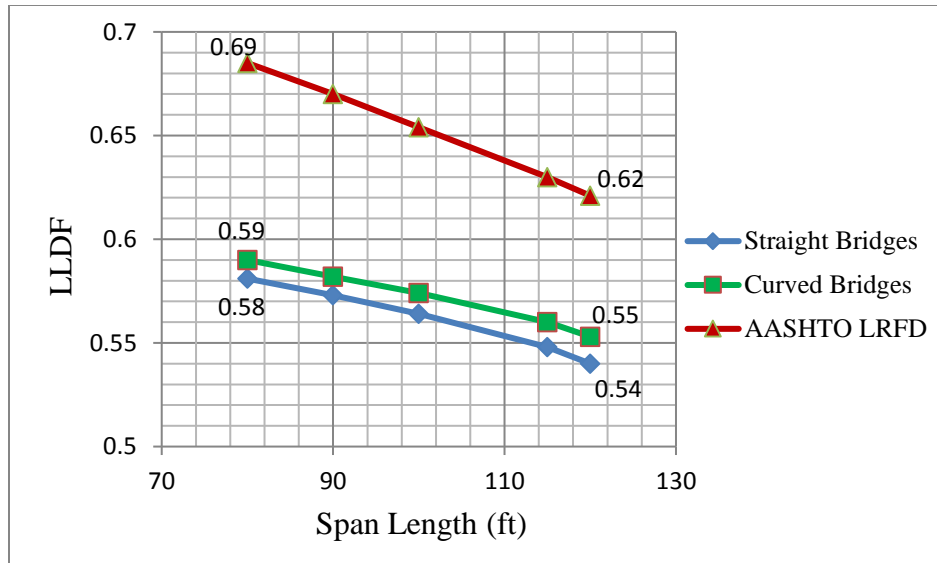


Figure 5.6: HL-93S- Two Lanes Loaded

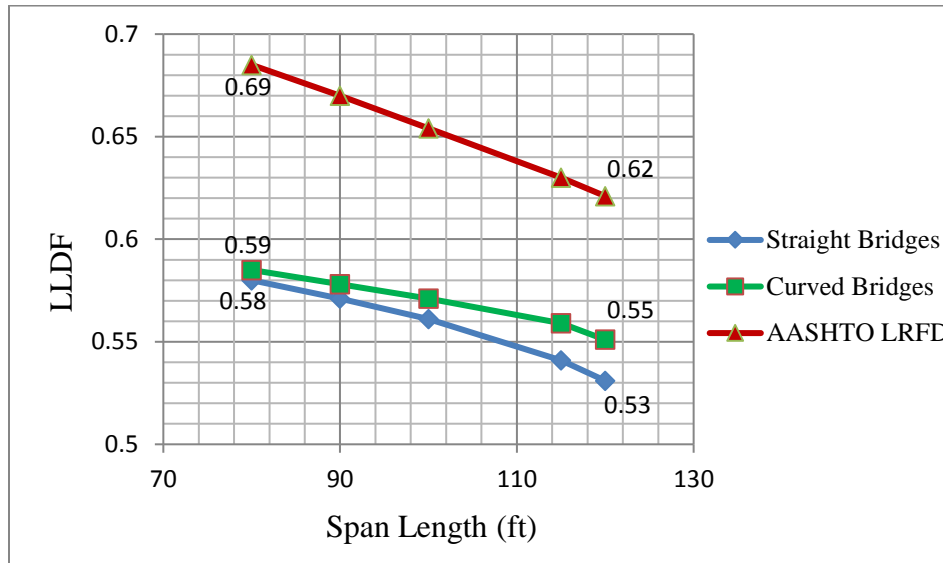


Figure 5.7: HL-93K- Two Lanes Loaded- Positive Moment

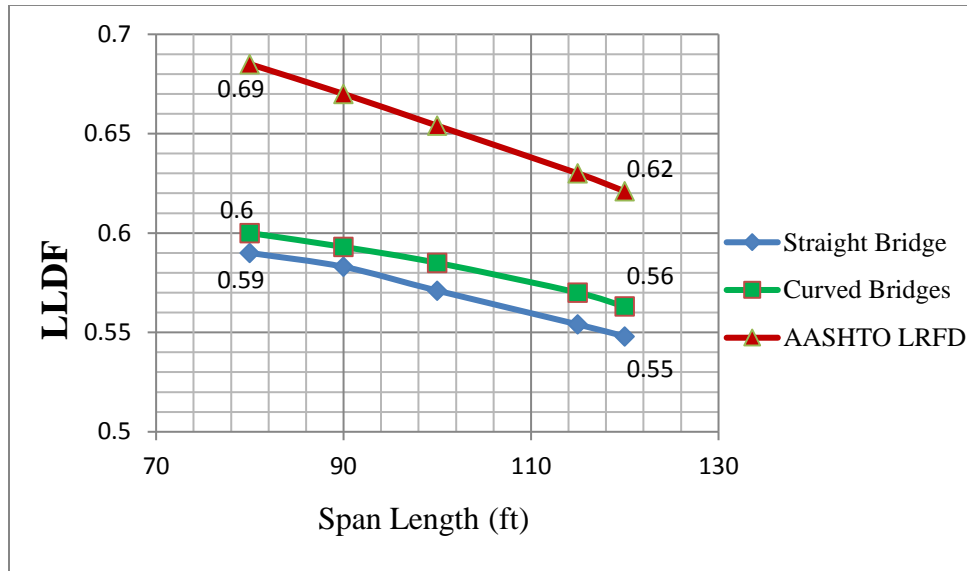


Figure 5.8: HL-93K- Two Lanes Loaded- Negative Moment

5.8 Distribution Factors for Central Angles of 38°, 45°, 50°, 55°, 60°

Tables 5.7-5.11 show the LLDF on curved bridges using HL-93K loading on two traffic lanes with a central angle equal to 38°, 45°, 50°, 55°, and 60°. These tables state the LLDF for interior girders that usually carry larger moments than those on exterior girders.

Table 5.7: LLDF for Curved Bridge with a Central Angle of 38°

LLDF for HL-93K- Two Lanes Loaded-Negative Moment		
Span Length (ft)	AASHTO LRFD	FEA Curved Bridge ($\theta = 38^\circ$)
80	0.69	0.71
90	0.67	0.69
100	0.65	0.67
115	0.63	0.64
120	0.62	0.63
140	0.60	0.61

Table 5.8: LLDF for Curved Bridge with a Central Angle of 45°

LLDF for HL-93K- Two Lanes Loaded-Negative Moment		
Span Length (ft)	AASHTO LRFD	FEA Curved Bridge ($\theta = 45^\circ$)
80	0.69	0.73
90	0.67	0.71
100	0.65	0.68
115	0.63	0.66
120	0.62	0.65
140	0.60	0.62

Table 5.9: LLDF for Curved Bridge with a Central Angle of 50°

LLDF for HL-93K- Two Lanes Loaded-Negative Moment		
Span Length (ft)	AASHTO LRFD	FEA Curved Bridge ($\theta = 50^\circ$)
80	0.69	0.74
90	0.67	0.72
100	0.65	0.70
115	0.63	0.67
120	0.62	0.66
140	0.60	0.63

Table 5.10: LLDF for Curved Bridge with a Central Angle of 55°

LLDF for HL-93K- Two Lanes Loaded-Negative Moment		
Span Length (ft)	AASHTO LRFD	FEA Curved Bridge ($\theta = 55^\circ$)
80	0.69	0.76
90	0.67	0.74
100	0.65	0.72
115	0.63	0.69
120	0.62	0.68
140	0.60	0.65

Table 5.11: LLDF for Curved Bridge with a Central Angle of 60°

LLDF for HL-93K- Two Lanes Loaded-Negative Moment		
Span Length (ft)	AASHTO LRFD	FEA Curved Bridge ($\theta = 60^\circ$)
80	0.69	0.79
90	0.67	0.77
100	0.65	0.75
115	0.63	0.72
120	0.62	0.71
140	0.60	0.67

5.9 Comparison of Results for Central angles of 38°, 45°, 50°, 55°, 60°

Figures 5.9-5.13 show the LLDF for curved bridge with different central angles (38°, 45°, 50°, 55°, 60°). The results were plotted for just greatest LLDF determined by maximum moments obtained from finite element analyses that accrued at negative

moment and two lanes loaded by the truck HL-93K. The result compared with the LLDF results that determined from AASHTO LLRDF for straight bridge (central angles = 0).

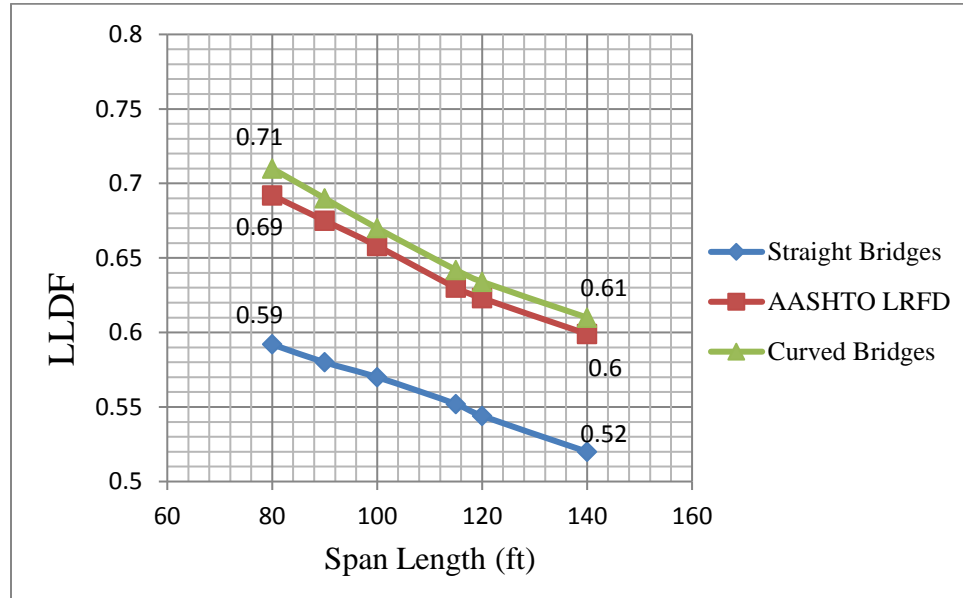


Figure 5.9: LLDF for Curved Bridge with a Central Angle of 38°

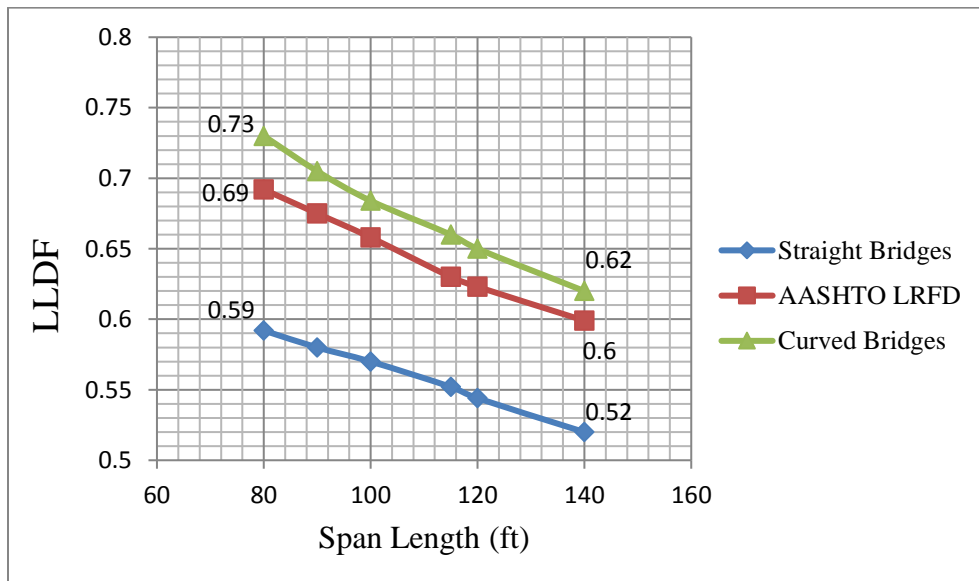


Figure 5.10: LLDF for Curved Bridge with a Central Angle of 45°

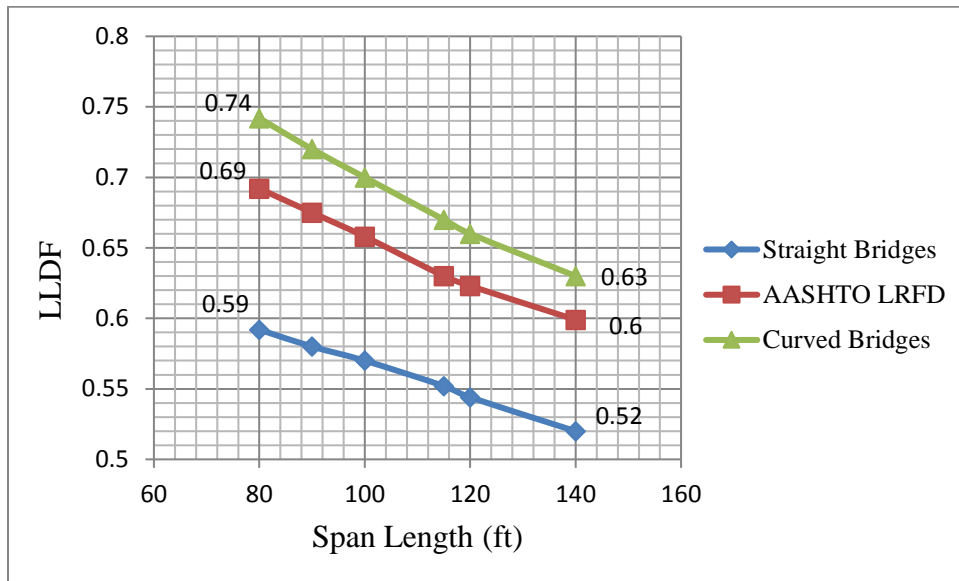


Figure 5.11: LLDF for Curved Bridge with a Central Angle of 50°

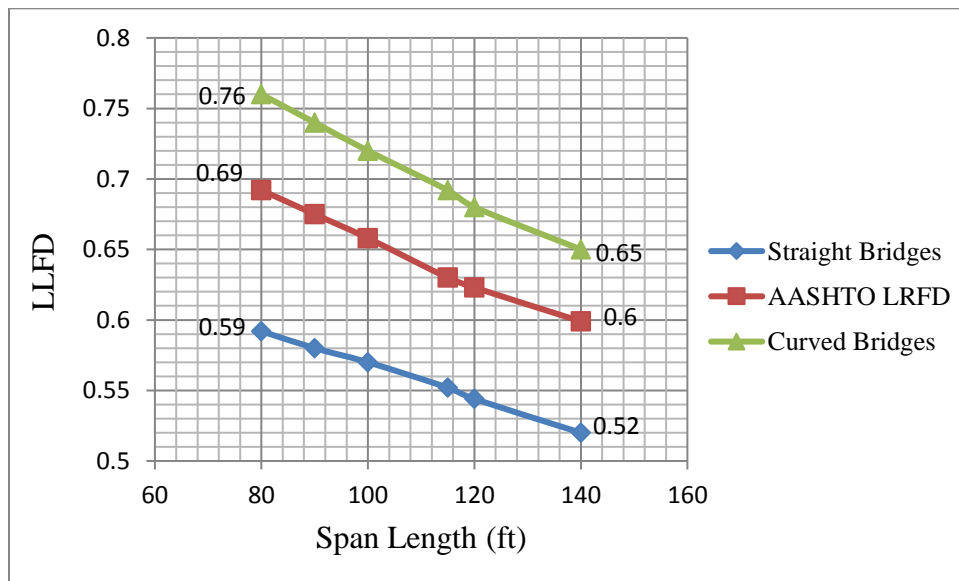


Figure 5.12: LLDF for Curved Bridge with a Central Angle of 55°

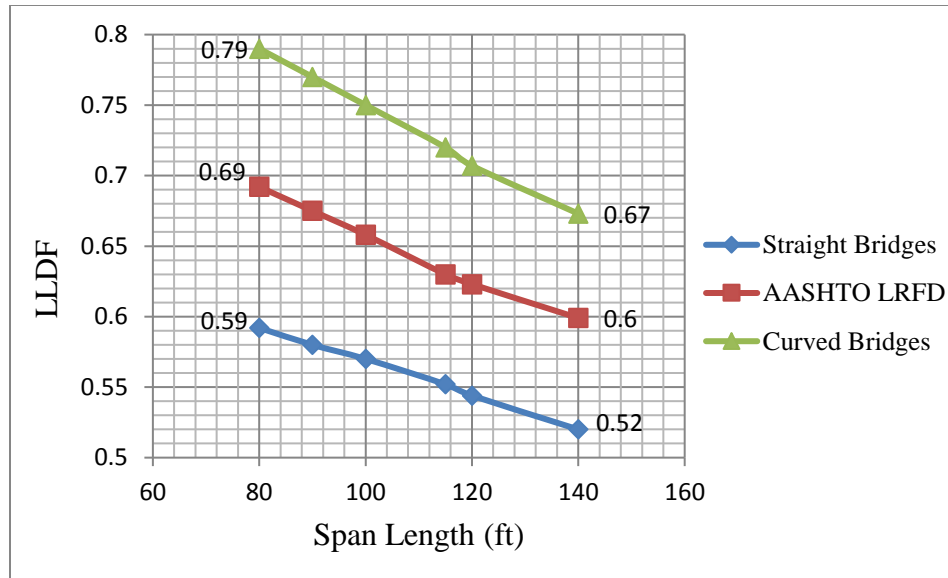


Figure 5.13: LLDF for Curved Bridge with a Central Angle of 60°

5.10 Distribution Factors for the Entire Bridge

Tables 5.12-5.16 show the Maximum LLDF for entire bridge (all girders). The entire superstructure is designed as a unit slab rather than as individual girders, AASHTO LRFD (4.6.2.2.1), [1] and WSDOT BDM [13].

Table 5.12: Maximum LLDF for the Entire Bridge

Curved Bridge ($\theta = 38^\circ$)					
Max LLDF on Individual Girder			Max LLDF on Entire Bridge		
Span Length (ft)	AASHTO LRFD	Interior Girder (Analysis)	Number of Webs	AASHTO LRFD	Interior Girder (Analysis)
80	0.69	0.71	4	2.76	2.84
90	0.67	0.69	4	2.70	2.76
100	0.65	0.67	4	2.61	2.60
115	0.63	0.64	4	2.52	2.57
120	0.62	0.63	4	2.50	2.54
140	0.60	0.61	4	2.40	2.44

Table 5.13: Maximum LLDF for the Entire Bridge

Curved Bridge ($\theta = 45^\circ$)					
Max LLDF on Individual Girder			Max LLDF on Entire Bridge		
Span Length (ft)	AASHTO LRFD	Interior Girder (Analysis)	Number of Webs	AASHTO LRFD	Interior Girder (Analysis)
80	0.69	0.73	4	2.76	2.92
90	0.67	0.71	4	2.70	2.82
100	0.65	0.68	4	2.61	2.74
115	0.63	0.66	4	2.52	2.64
120	0.62	0.65	4	2.50	2.60
140	0.60	0.62	4	2.40	2.48

Table 5.14: Maximum LLDF for the Entire Bridge

Curved Bridge ($\theta = 50^\circ$)					
Max LLDF on Individual Girder			Max LLDF on Entire Bridge		
Span Length (ft)	AASHTO LRFD	Interior Girder (Analysis)	Number of Webs	AASHTO LRFD	Interior Girder (Analysis)
80	0.69	0.74	4	2.76	2.97
90	0.67	0.72	4	2.70	2.88
100	0.65	0.70	4	2.61	2.80
115	0.63	0.67	4	2.52	2.68
120	0.62	0.66	4	2.50	2.64
140	0.60	0.63	4	2.40	2.52

Table 5.15: Maximum LLDF for the Entire Bridge

Curved Bridge ($\theta = 55^\circ$)					
Max LLDF on Individual Girder			Max LLDF on Entire Bridge		
Span Length (ft)	AASHTO LRFD	Interior Girder (Analysis)	Number of Webs	AASHTO LRFD	Interior Girder (Analysis)
80	0.69	0.76	4	2.76	3.04
90	0.67	0.74	4	2.7	2.96
100	0.65	0.72	4	2.61	2.88
115	0.63	0.69	4	2.52	2.77
120	0.62	0.68	4	2.50	2.72
140	0.60	0.65	4	2.40	2.60

Table 5.16: Maximum LLDF for the Entire Bridge

Curved Bridge ($\theta = 60^\circ$)					
Max LLDF on Individual Girder			Max LLDF on Entire Bridge		
Span Length (ft)	AASHTO LRFD	Interior Girder (Analysis)	Number of Webs	AASHTO LRFD	Interior Girder (Analysis)
80	0.69	0.79	4	2.76	3.16
90	0.67	0.77	4	2.70	3.08
100	0.65	0.75	4	2.61	3.00
115	0.63	0.72	4	2.52	2.88
120	0.62	0.71	4	2.50	2.83
140	0.60	0.67	4	2.40	2.69

5.11 LLDF Values with the Effects of CE and BR Forces

Tables 5.17- 5.21 and Figures 5.14-5.18 show the indirect LLDF results for different central angles with including the effects of centrifugal and braking forces. Also, the results of indirect LLDF along with span lengths were plotted for just greatest indirect LLDF determine through the maximum moments obtained from 3-D modeling analyses that accrued at negative moment and two lanes loaded by the truck HL-93K. The result compared with the LLDF results that determined from AASHTO LLRDF for straight bridge. The results of greatest maximum moments for different span lengths and central angles are attached in Appendix A.

Table 5.17: Indirect LLDF with a Central Angle of 38° Including CE and BR Force Effects

LLDF for HL-93K- Two Lanes Loaded-Negative Moment			
Span Length (ft)	AASHTO LRFD	FEA Curved Bridge ($\theta = 38^\circ$)	Including the Effect of Braking and Centrifugal Forces
			FEA Curved Bridge ($\theta = 38^\circ$)
80	0.69	0.71	0.89
90	0.67	0.69	0.87
100	0.65	0.67	0.85
115	0.63	0.64	0.83
120	0.62	0.63	0.82
140	0.62	0.61	0.79

Table 5.18: Indirect LLDF with a central angle of 45° including CE and BR force effects

LLDF for HL-93K- Two Lanes Loaded-Negative Moment			
Span Length (ft)	AASHTO LRFD	FEA Curved Bridge ($\theta = 45^\circ$)	Including the Effect of Braking and Centrifugal Forces
			FEA Curved Bridge ($\theta = 45^\circ$)
80	0.69	0.73	0.93
90	0.67	0.71	0.91
100	0.65	0.68	0.88
115	0.63	0.66	0.85
120	0.62	0.65	0.84
140	0.62	0.62	0.82

Table 5.19: Indirect LLDF with a Central Angle of 50° Including CE and BR Force Effects

LLDF for HL-93K - Two Lanes Loaded-Negative Moment			
Span Length (ft)	AASHTO LRFD	FEA Curved Bridge ($\theta = 50^\circ$)	Including the Effect of Braking and Centrifugal Forces
			FEA Curved Bridge ($\theta = 50^\circ$)
80	0.69	0.74	0.97
90	0.67	0.72	0.95
100	0.65	0.7	0.93
115	0.63	0.67	0.89
120	0.62	0.66	0.88
140	0.62	0.63	0.84

Table 5.20: Indirect LLDF with a Central Angle of 55° Including CE and BR Force Effects

LLDF for HL-93K- Two Lanes Loaded-Negative Moment			
Span Length (ft)	AASHTO LRFD	FEA Curved Bridge ($\theta = 55^\circ$)	Including the Effect of Braking and Centrifugal Forces
			FEA Curved Bridge ($\theta = 55^\circ$)
80	0.69	0.76	1.03
90	0.67	0.74	1.00
100	0.65	0.72	0.98
115	0.63	0.69	0.94
120	0.62	0.68	0.93
140	0.62	0.65	0.90

Table 5.21: Indirect LLDF with a Central Angle of 60° Including CE and BR Force Effects

LLDF for HL-93K- Two Lanes Loaded-Negative Moment			
Span Length (ft)	AASHTO LRFD	FEA Curved Bridge ($\theta = 60^\circ$)	Including the Effect of Braking and Centrifugal Forces
			FEA Curved Bridge ($\theta = 60^\circ$)
80	0.69	0.79	1.05
90	0.67	0.77	1.02
100	0.65	0.75	1.00
115	0.63	0.72	0.96
120	0.62	0.71	0.95
140	0.62	0.67	0.92

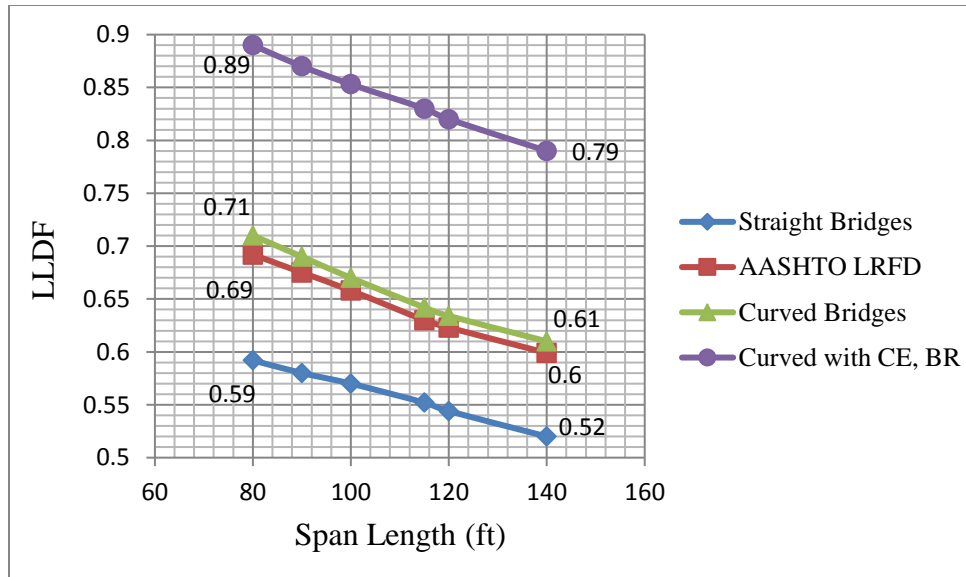


Figure 5.14: LLDF for Curved Bridge with a Central Angle of 38°

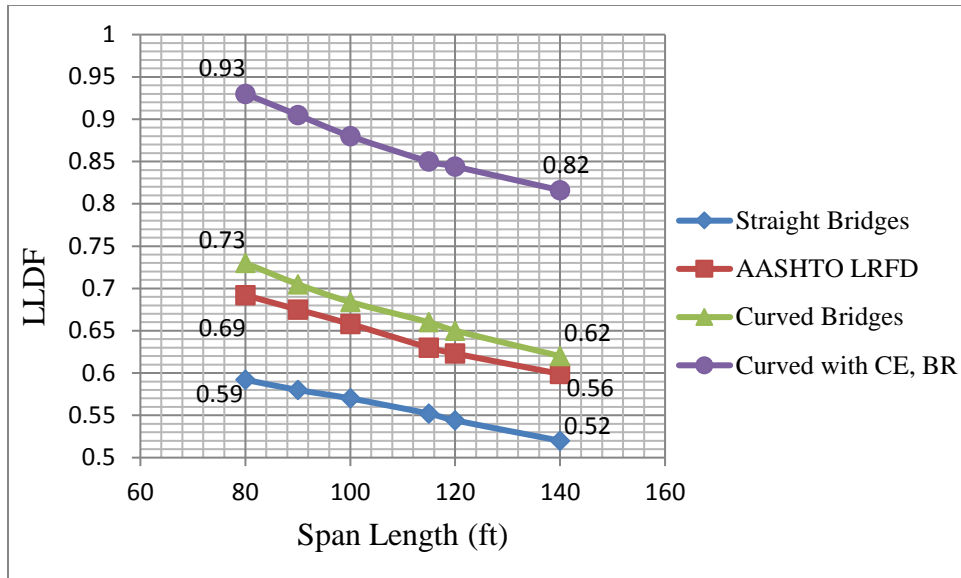


Figure 5.15: LLDF for Curved Bridge with a Central Angle of 45°

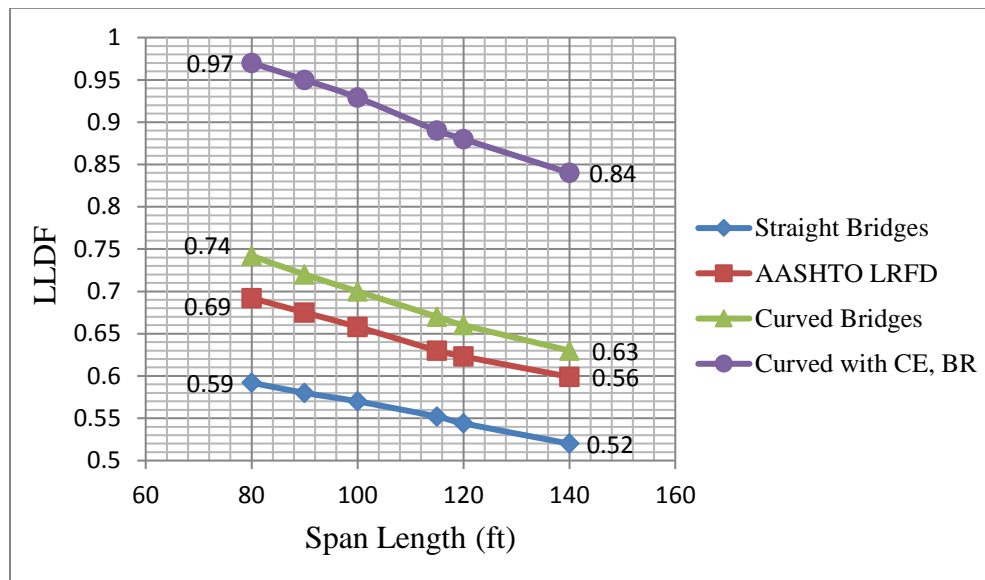


Figure 5.16: LLDF for Curved Bridge with a Central Angle of 50°

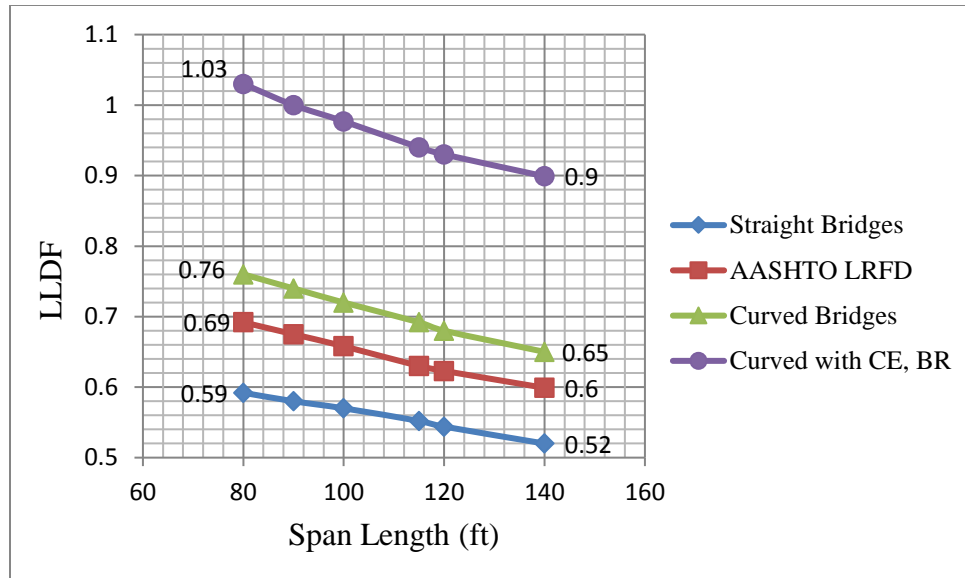


Figure 5.17: LLDF for Curved Bridge with a Central Angle of 55°

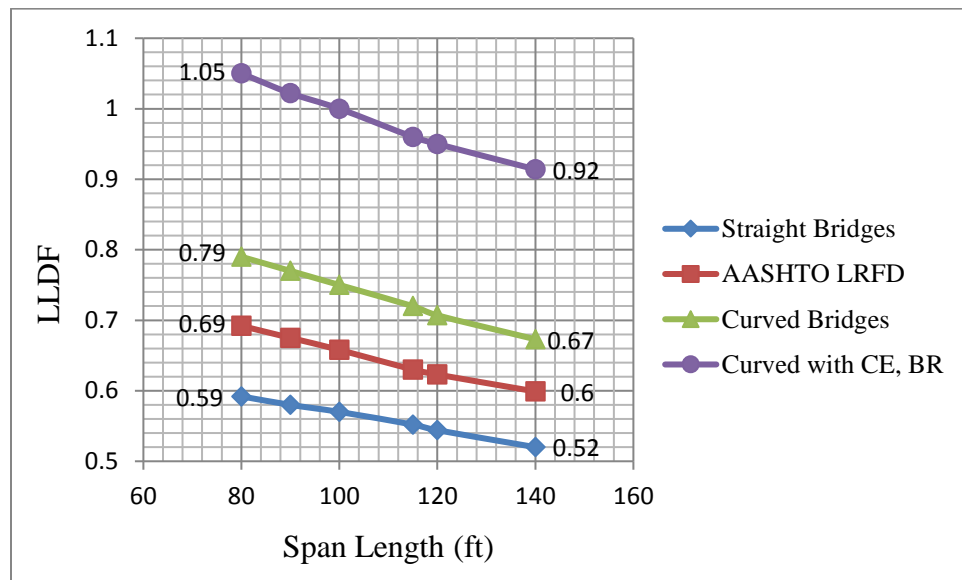


Figure 5.18: LLDF for Curved Bridge with a Central Angle of 60°

Chapter six (6) of this study includes the summary and conclusions for straight bridges and for curved bridges that were affected and not affected by centrifugal (CE) and braking (BR) forces.

CHAPTER 6

SUMMARY AND CONCLUSIONS

6.1 Summary

6.1.1 Straight Box Girder Bridges

Consistent with the AASTHO LRFD, the magnitude of the distribution factors that obtained from finite element analysis decreases with an increase in span length. Since the longitudinal stiffness is found to be related to the span length (L). The general trend of the relationship is the stiffness increases as span length increases. That leads to decrease the stress which in turn leads to decrease the distribution factors. The results show that distribution factors from the refined analysis are smaller than those calculated from the LRFD formula. Results indicate that the current LRFD specifications distribution factor formulas for box-girder bridges generally provide a conservative estimate of the design bending moment. Distribution factors are generally more conservative for exterior girders than for interior girders. Also, the LLDF obtained from both the analyses and AASHTO LRFD for one design lane loaded is less than two lanes loaded for all cases mentioned before. In addition, the LRFD specification distribution factor became less conservative with an increase in span length for both girder types.

6.1.2 Curved Box Girder Bridges

The AASHTO LRFD Design Specifications provide a set of live load distribution factor formulas for determining the distribution of bending moment effects in both the interior and exterior girders of highway bridges. However, there are limitations on the use of these distribution factors, such as the central angle that is limited up to 34° . As a result, refined analyses using 3D models are required to design bridges outside of these limits.

The analyses of various curved box girder models are carried out in CSiBridge software by varying span lengths and central angles. The models are conducted by varying the span lengths while the angle of curvature is kept constant. From the results obtained after the analysis of curved box girder, the following conclusions are made.

- ❖ LLDFs decrease with an increase of span lengths within the same central angle. That is because the effect of the curvature goes down as the radius of curvature goes up, due to the increase in span lengths. Also, the stiffness of girders increases as the span length increases, as pointed out before.
- ❖ It is observed from a refined analysis that the distribution factor increases as the curvature of box girder increases. Using a span length of 80 ft. as an example, the LLDF for a straight bridge is 0.69 from LRFD's formula and 0.73 from a refined analysis, with a central angle of 45° . The percentage difference is about 6%, even though a 45° angle is quite far away from the limits of the LRFD specification (34°).
- ❖ The value of LLDFs that are determined from an analysis for a central angle of 38° is a little higher than those obtained from LRFD equations for straight bridges. Therefore, AASHTO LRFD formulas can be used for curved box girder

bridges up to its limits of 34° central angle or even until a little outside of the LRFD limits. Also, these values of LLDF state that the distribution factor formulas for box-girder bridges obtained from the current AASHTO LRFD provide a conservative LLDF due to the bending moment.

- ❖ The distribution factor for curved bridges with a central angle of 5° does not vary significantly with the LLDF obtained from the analysis for straight bridges.

6.2 Conclusions

6.2.1 Straight Bridge

- ❖ The results indicate that the current AASHTO LRFD formulas for box-girder bridges provide a conservative estimate of the design bending moment.
- ❖ Live load distribution factors obtained from LRFD for exterior girders are generally more conservative than that for interior girders.

6.2.2 Curved Bridge

- ❖ It was observed from a refined analysis that the distribution factor increases as the central angle increases.
- ❖ The current AASHTO LRFD formulas for multi-cell box girder bridges are applicable for curved bridges that have central angles up to 34° or even until 38°, which is a little out of the LRFD's limits.
- ❖ The maximum moment on the exterior girders increases very significantly due to the effect of centrifugal and braking forces. And, the bending moment generally increases under the braking force.

- ❖ The results of LLDF for a prismatic curved box girder bridge for different central angles and span lengths are tabled and plotted. These results provide distribution factors that can be used by engineering designers to design these kinds of bridges. That are useful and more realistic because those analyses have been conducted for real box girder bridge geometry.

APPENDIX

RESULTS OF MOMENTS

Tables A.1-A.6 show the results of maximum moments due to trucks HL-93K and HL-93S for straight bridges for each individual case. Tables A.7-A.12 state the moment results for curved bridges for different span lengths and central angles. These results represent the greatest negative moments that occurred due to HL-93K, two lanes loaded, and for interior girder 1 (Fig A.1). Tables A.13-A.17 indicate the results of maximum moments for curved bridges that included the effects of centrifugal and braking forces. These values resulted in the highest LLDF for negative moment generated by the HL-93K loading, two lanes loaded, and for left exterior girder (Fig A.1), as the greatest moment occurs on the exterior girder as a result of the effect of centrifugal force.

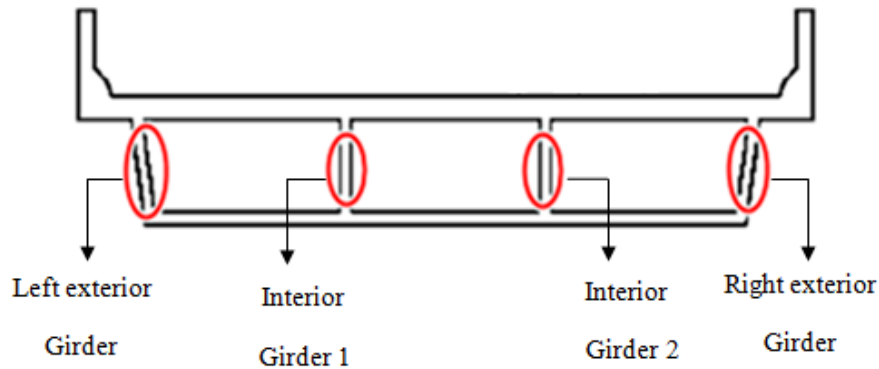


Figure A.1: Description of Interior and Exterior Girders

Table A.1: Results of Negative Moments (Kips-ft) for HL-93S- One Lane Loaded

Span Length (ft)	Entire Bridge	Interior Girder (1)	Interior Girder (2)	Left Exterior Girder	Right Exterior Girder
80	1998	600	655	320	591
90	2367	685	760	405	694
100	2738	765	850	499	790
115	3321	855	998	641	925
120	3525	915	1035	701	980
140	4376	1110	1240	908	1179

Table A.2: Results of Negative Moments (Kips-ft) for HL-93S- Two Lanes Loaded

Span Length (ft)	Entire Bridge	Interior Girder (1)	Interior Girder (2)	Left Exterior Girder	Right Exterior Girder
80	3331	967	967	700	700
90	3945	1131	1131	895	895
100	4564	1280	1280	1056	1056
115	5536	1530	1530	1290	1290
120	5875	1590	1590	1389	1389
140	7292	1910	1910	1725	1725

Table A.3: Results of Positive Moments (Kips-ft) for HL-93K- One Lane Loaded

Span Length (ft)	Entire Bridge	Interior Girder (1)	Interior Girder (2)	Left Exterior Girder	Right Exterior Girder
80	1961	525	616	370	550
90	2333	625	713	450	600
100	2709	710	795	550	682
115	3305	835	940	692	800
120	3510	890	960	750	850
140	4368	1060	1150	965	1025

Table A.4: Results of Negative Moments (Kips-ft) for HL-93K- One Lane Loaded

Span Length (ft)	Entire Bridge	Interior Girder (1)	Interior Girder (2)	Left Exterior Girder	Right Exterior Girder
80	1425	410	470	230	430
90	1699	475	550	290	500
100	1996	550	625	367	580
115	2473	638	748	478	691
120	2641	680	770	505	746
140	3361	854	920	690	935

Table A.5: Results of Positive Moments (Kips-ft) for HL-93K- Two Lanes Loaded

Span Length (ft)	Entire Bridge	Interior Girder (1)	Interior Girder (2)	Left Exterior Girder	Right Exterior Girder
80	3269	948	948	724	724
90	3888	1109	1109	860	860
100	4597	1295	1295	1040	1040
115	5600	1550	1550	1270	1270
120	6007	1600	1600	1389	1389
140	7280	1830	1830	1711	1711

Table A.6: Results of Negative Moments (Kips-ft) for HL-93K- Two Lanes Loaded

Span Length (ft)	Entire Bridge	Interior Girder (1)	Interior Girder (2)	Left Exterior Girder	Right Exterior Girder
80	2374	700	700	550	550
90	2831	818	818	652	652
100	3376	960	960	780	780
115	4284	1197	1197	995	995
120	4539	1255	1255	1062	1062
140	5602	1460	1460	1320	1320

Table A.7: Results of Negative Moments for Curved Bridges with a Central Angle of 5°

Negative Moments (Kips-ft) Due to HL-93K- Two Lanes Loaded		
Span Length (ft)	Entire Bridge	Interior Girder (1) Curved Bridge ($\theta = 5^\circ$)
80	2484	745
90	3016	888
100	3510	1015
115	4404	1250
120	4662	1303

Table A.8: Results of Negative Moments for Curved Bridges with a Central Angle of 38°

Negative Moments (Kips-ft) Due to HL-93K- Two Lanes Loaded		
Span Length (ft)	Entire Bridge	Interior Girder (1) Curved Bridge ($\theta = 38^\circ$)
80	2780	986
90	3305	1140
100	3918	1312
115	4822	1542
120	5160	1625
140	6530	1991

Table A.9: Results of Negative Moments for Curved Bridges with a Central Angle of 45°

Negative Moments (Kips-ft) Due to HL-93K- Two Lanes Loaded		
Span Length (ft)	Entire Bridge	Interior Girder (1) Curved Bridge ($\theta = 45^\circ$)
80	2925	1067
90	3440	1221
100	4009	1363
115	5040	1663
120	5345	1737
140	6680	2070

Table A.10: Results of Negative Moments for Curved Bridges with a Central Angle of 50°

Negative Moments (Kips-ft) Due to HL-93K- Two Lanes Loaded		
Span Length (ft)	Entire Bridge	Interior Girder (1) Curved Bridge ($\theta = 50^\circ$)
80	2978	1102
90	3514	1265
100	4146	1451
115	5126	1717
120	5447	1797
140	6787	2138

Table A.11: Results of Negative Moments for Curved Bridges with a Central Angle of 55°

Negative Moments (Kips-ft) Due to HL-93K- Two Lanes Loaded		
Span Length (ft)	Entire Bridge	Interior Girder (1) Curved Bridge ($\theta = 55^\circ$)
80	3080	1170
90	3622	1340
100	4275	1539
115	5300	1829
120	5620	1911
140	7018	2281

Table A.12: Results of Negative Moments for Curved Bridges with a Central Angle of 60°

Negative Moments (Kips-ft) Due to HL-93K- Two Lanes Loaded		
Span Length (ft)	Entire Bridge	Interior Girder (1) Curved Bridge ($\theta = 60^\circ$)
80	3190	1260
90	3771	1452
100	4452	1670
115	5520	1987
120	5870	2084
140	7235	2424

Table A.13: Results of Negative Moments for Curved Bridges with a Central Angle of 38°

Negative Moments (Kips-ft) Due to HL-93K- Two Lanes Loaded Including the Effects of Centrifugal and Braking Forces		
Span Length (ft)	Entire Bridge	Interior Girder (1) Curved Bridge ($\theta = 38^\circ$)
80	3280	1460
90	3746	1630
100	4400	1870
115	5080	2108
120	5672	2328
140	6500	2580

Table A.14: Results of Negative Moments for Curved Bridges with a Central Angle of 45°

Negative Moments (Kips-ft) Due to HL-93K- Two Lanes Loaded Including the Effects of Centrifugal and Braking Forces		
Span Length (ft)	Entire Bridge	Interior Girder (1) Curved Bridge ($\theta = 45^\circ$)
80	3672	1705
90	4060	1850
100	4600	2050
115	5300	2250
120	6160	2580
140	6910	2840

Table A.15: Results of Negative Moments for Curved Bridges with a Central Angle of 50°

Negative Moments (Kips-ft) Due to HL-93K- Two Lanes Loaded Including the Effects of Centrifugal and Braking Forces		
Span Length (ft)	Entire Bridge	Interior Girder (1) Curved Bridge ($\theta = 50^\circ$)
80	3800	1840
90	4600	2180
100	5292	2460
115	6200	2755
120	6705	3950
140	7324	3080

Table A.16: Results of Negative Moments for Curved Bridges with a Central Angle of 55°

Negative Moments (Kips-ft) Due to HL-93K- Two Lanes Loaded Including the Effects of Centrifugal and Braking Forces		
Span Length (ft)	Entire Bridge	Interior Girder (1) Curved Bridge ($\theta = 55^\circ$)
80	4174	2150
90	5010	2500
100	5664	2780
115	6590	3093
120	7007	3260
140	8116	3650

Table A.17: Results of Negative Moments for Curved Bridges with a Central Angle of 60°

Negative Moments (Kips-ft) Due to HL-93K- Two Lanes Loaded Including the Effects of Centrifugal and Braking Forces		
Span Length (ft)	Entire Bridge	Interior Girder (1) Curved Bridge ($\theta = 60^\circ$)
80	4800	2520
90	5865	2990
100	6100	3045
115	7090	3400
120	7610	3615
140	8570	3940

BIBLIOGRAPHY

- [1] AASHTO (2012). *AASHTO LRFD Bridge Design Specification*, 6th Edition, American Association of State Highway and Transportation Officials, Washington, D.C.
- [2] South Carolina Department of Transportation (SCDOT). "Structural Analysis and Evaluation." *Bridge Design Manual*, Chapter. 14, 2006.
- [3] Zokaie, Toorak. "AASHTO- LRFD Live Load Distribution Specifications." *Journal of Bridge Engineering*, Vol.5, No. 2 (2000), pp. 131-138.
- [4] Barr, Paul., Stanton, John., and Eberhard, Marc. "Live Load Distribution Factors for Washington State". Chapter. 2, 2000.
- [5] Aswad, Alex., and Chen, Yohchia. "Impact of LRFD Specifications on Load Distribution of Prestressed Concrete Girders." *PCI Journal*, Vol. 39, No. 5 (1994), pp. 78-89.
- [6] Chen, Yohchia., and Aswad, Alex. "Stretching Span Capability of Prestressed Concrete Bridges Under AASHTO LRFD." *Journal of Bridge Engineering*, Vol. 1, No. 3 (1996), pp. 112-120.
- [7] Shahawy, Mohsen., and Huang, Dongzhou. "Analytical and Field Investigation of Lateral Load Distribution in Concrete Slab-On-Girder Bridges." *ACI Structural Journal*, Vol. 98, No. 4 (2001), pp. 590-599.
- [8] Smith, David. "Force Effects in Slab-on-Girder Bridge Types at Ultimate and Serviceability Limit States and Recommendations for Live Load Distribution Factors for the Canadian Highway Bridge Design Code." Volumes 1 and 2, *Report for New Brunswick Department of Transportation*, 1996.
- [9] Khaleel, Mohammad., and Itani, Rafik. "Live- Load Moments for Continuous Skew Bridges." *Journal of Structural Engineering*, Vol. 116, No. 9 (1990), pp. 2361-2373.
- [10] Zokaie, Toorak., Osterkamp, Timothy., and Imbsen, Roy. *Distribution of Wheel Loads on Highway Bridges*. Natinal Cooperative Highway Research Program (NCHRP), Report 12-26, Transportation Research Board, Washington, D.C, 1991.

- [11] Barker, Richard., and Puckett, Jay. *Design of Highway Bridges An LRFD Approach*. Published by John Wiley and Sonns Inc, 3th Edition, New Jersey, 2013.
- [12] CSiBridge (2015). *Computer and Structure Inc*, Version. 15, Structural and Earthquake Engineering Software, Analysis Reference Manual.
- [13] Washington State Department of Transportation. "WSDOT Bridge Design Manual (LRDF)." *Bridge and Structure Office*, Chapter. 5, 2015.
- [14] Sasidharan, Nila., and Johny, Basil. "Finite Element Analysis and Parametric Study of Curved Concrete Box Girder Using Abaqus Software." *International Journal of Research in Enginnering and Technology*, Vol. 4, No.10 (2015), pp. 425-429.
- [15] Song, Shin., Chai, Y., and Hida, Susan. "Live-Load Distribution Factors for Concrete Box-Girder Bridges." *Journal of Bridge Engineering*, Vol. 8, No. 5 (2003), pp. 273-280.
- [16] Sotelino, Elisa., Liu, Judy., Chung, Wonseok., and Phuvoravan, Kitjapat. *Simplified Load Distribution Factor for Use in LRFD Design*. Prepared in cooperation with the Indiana Department of Transportation and the US Department of Transportation Fedral Highway Administration, 2004.
- [17] Tobias, Daniel. "Perspective on AASHTO Load and Resistance Facto Design." *Journal of Bridge Engineering*, Vol. 16, No. 6 (2011), pp. 684-692.
- [18] State of Connecticut Department of Transportation. "BRIDGE DESIGN MANUAL." Section. 6, 2003.
- [19] Sennah, Khaled., and Kennedy, John. "Load Distribution Factors For Composite Multicell Box Girder Bridges." *Journal of Bridge Engineering*, Vol. 4, No. 1 (1999), pp. 71-78.
- [20] Sayhood, Eyad., Khaled, Raid., and Hassan, Hashim. "Load Distribution Factors for Horizontally Curved Concrete Box Girder Bridges." *Engineering and Technology Journal*, Vol. 32, part A (2014), pp.748-762.
- [21] Sarode,Ashish., and Vesmawala GR. "Parametric Study of Horizontally Curved Box Girders for Torsional Behavior and Stability." *International Refereed Journal of Engineering and Science (IRJES)*, Vol. 3, No. 2 (2014), pp. 50-55.
- [22] Samaan, Magdy., Sennah, Khaled., and Kennedy, John. "Distribution of Wheel Loads on Continuous Steel Spread-Box Girder Bridges." *Journal of Bridge Engineering*, Vol. 7, No. 3 (2002), pp. 175-183.

- [23] ASHTO (2001). *A Policy Geometric Design of Highways and Street*, 4th Edition, American Association of State Highway and Transportation Officials, Washington, DC.
- [24] Samaan, Magdy., Sennah, Khaled., and Kennedy, John. "Distribution Factors for Curved Continuous Composite Box-Girder Bridges." *Journal of Bridge Engineering*, Vol. 10, No. 6 (2005), pp. 678-692.
- [25] Nowak, Andrzej. "Calibration of LRFD Bridge Code." *Journal of Structural Engineering*, Vol. 121, No.8 (1995), pp.1245-1251.
- [26] Gouda, Laxmi. *STUDY ON PARAMETRIC BEHAVIOUR OF SINGLE CELL BOX GIRDER UNDER DIFFERENT RADIUS OF CURVATURE*. A thesis submitted to Department of Civil Engineering, National Institute of Technology Rourkela, Odisha, India, 2013.
- [27] Kim, Yail., Tonovic, Rusmir., and Wight Gordon. *Applicability of AASHTO LRFD Live Load Distribution Factors for Nonstandard Truck Load*. Challenges, Opportunities and Solution in Structural Engineering and Construction, Taylor & Francis Group, London, 2010.
- [28] Kim, Woo., Laman, Jeffrey., and Linzell, Daniel. "Live Load Radial Moment Distribution for Horizontally Curved Bridges." *Journal of Bridge Engineering*, Vol. 12, No. 6 (2007), pp. 727-736.
- [29] Hodson, D., Barr, P., and Halling, M. "Live- Load Analysis of Posttensioned Box-Girder Bridges." *Journal of Bridge Engineering*, Vol. 17, No. 4 (2012), pp. 644-651.
- [30] Doust, Saeed. *Extending Integral Concepts to Curved Bridge Systems*. A dissertation submitted to university of Nebraska, 2011.
- [31] Sivakumar, Bala., and Ghosn, Michel. *Recalibration of LRFR Live Load Factors in the AASHTO Manual for Bridge Evaluation*. Prepared for the National Cooperative Highway Research Program (NCHRP), Project 20-07, 2011.
- [32] Hughs, Erin., and Idriss, Rola. "Live-Load Distribution Factors for Prestressed Concrete, Spread Box-Girder Bridge." *Journal of Bridge Engineering*, Vol. 11, No. 4 (2006), pp.573-581.
- [33] Ibrahim, Manal. *Investigation of Load Distribution Factors for Two-Span Continuous Composite Multiple Box girder Bridges*. A thesis presented to Ryerson University, 2012.

- [34] Li, Jingjuan., and Chen, Genmiao. *Method to Compute Live-Load Distribution in Bridge Girders*. Practice Periodical on Strutural Design and Construction, 2011.
- [35] National Cooperative Highway Research Program (NCHRP). *Simplified Live Load Distribution Factor Equations*. Transportation Research Board of the National Academies, Report 592, 2007.
- [36] Linzell, Daniel., and other. Abner Chen, Mohammed Shrafbayani, Junwon Seo, Deanna Nevling, Tanit Jaissa, Omer Ashour: *Guidelines for Analyzing Curved and Skewed Bridges and Designing Them for Construction*. Pennsylvania Department of Transportation, 2010.
- [37] Pockels, Leonardo. *Live-Load Test and Computer Modeling of a Pre- Cast Concrete Deck, Steel Girder Bridge, and a Cast-in-Place Concrete Box Girder Bridge*. A thesis submitted to Civil and Enviromental Engineeering, Utah State Univeridty, 2009.
- [38] Tiedeman, Jane., and Albrecht, Pedro. “Behavior of Two-Span Continuous Bridge Under Truck Axial Loading.” *Journal of Structural Engineering*. Vol. 119, No. 4 (1993), pp. 1234-1250.
- [39] Hall, Dann., Grubb, Micheal., and Yoo, Chain. *Improved Design Specifications for Horizontally Curved Steel Girder Highway Bridges*. Prepared by National Cooperative Highway Research Program (NCHRP), Transportation Research Board, Project 12-38, 1998.
- [40] Nowak, Andrzej. “Live Load Model for Highway Bridges.” *Journal of Structural Safety*, Vol. 13, Nos. 1 and 2 (1993), pp. 53-66.